https://doi.org/10.5194/egusphere-2024-694
Preprint. Discussion started: 16 April 2024


# Developing the DO3SE-crop model for Xiaoji, China

Pritha Pande[1]; Sam Bland[1]; Nathan Booth [2];Jo Cook[2]; Zhaozhong Feng[3]; Lisa Emberson[2].

[1] Stockholm Environment Institute at York, Environment & Geography Dept., University of York, YO10 5DD, UK

[2] Environment & Geography Dept., University of York, YO10 5DD,UK

[3] Key Laboratory of Agrometeorology of Jiangsu Province, School of Ecology and Applied Meteorology, Nanjing University of Information Science & Technology, Nanjing, China.

Correspondence to: Pritha Pande (pritha.pande@york.ac.uk)

## Abstract

A substantial body of empirical evidence exists to suggest that elevated $O_3$ levels are causing significant impacts on wheat yields at sites representative of highly productive arable regions of ufor risk assessment) to incorporate a coupled $A_{net}$-$g_{sto}$ model to estimate $O_3$ uptake, an $O_3$ damage module (that impacts instantaneous $A_{net}$ and the timing and rate of senescence), and a crop phenology, carbon allocation and growth model based on the JULES-Crop model. The model structure allows scaling from the leaf to the canopy to allow for multiple leaf populations and canopy layers. The $DO_3SE$-crop model is calibrated and parametrised using $O_3$ fumigation data from Xiaoji, China for the year 2008 and for an $O_3$ tolerant and sensitive cultivar. The calibrated model can simulate key physiological variables, crop development, and yield with a good level of accuracy compared to experimental observations. $DO_3SE$-crop accurately depicted the difference in yield reductions under ambient and elevated $O_3$ treatments for wheat cultivars Y16 (tolerant) and Y2 (sensitive) with regressions of modelled and observed absolute yields resulting in an $R^2$ of 0.99 and an RMSE of 9.27 g/m². Further, when evaluated for 2007 and 2009 for all cultivars, the $DO_3SE$-crop model simulated O3-induced yield losses of 4-25% compared to observed yield losses of 12-34%, with an $R^2$ of 0.73 and an RMSE of 58.41 g/m². Additionally, our results indicate that the variance in yield reduction is primarily attributed to the premature decrease in carbon assimilation to the grains under elevated $O_3$ exposure. This is linked to accelerated leaf senescence, which brings leaf senescence forward by 7-9 days under elevated $O_3$ treatments.

https://doi.org/10.5194/egusphere-2024-694
Preprint. Discussion started: 16 April 2024


## Introduction

Ground-level ozone ($O_3$) is considered the most critical air pollutant causing global damage to crops. Elevated $O_3$ concentrations are particularly problematic in Asia, where decades of rapid economic growth, industrialisation, and urbanisation have seen sharp rises in pollutant emissions associated with burning fossil fuels (Lin *et al.*, 2017). At the same time, climate change is considered a substantial threat to arable productivity through changes in average and extreme temperature and precipitation profiles across the region (IPCC, 2007 & 2014). Reductions in precipitation are considered responsible for poor harvests in recent years (Liu *et al.*, 2010), and rising temperatures that reduce the length of the crop growing season are thought to have caused losses in crop yield (Malhi, Kaur and Kaushik, 2021).There is now substantial evidence showing that stresses from ozone pollution and climate variability interact, causing either additive, synergistic, or antagonistic responses in crop development, growth, and yield (Sillmann *et al.*, 2021). The threat posed by these stresses is a particular cause for concern in Asia since the continent contributes approximately 43% of the global wheat production, with China contributing the highest production levels at 17% (Feng *et al.*, 2021). $O_3$ levels are rising substantially in important wheat-growing areas in China such as the North China Plain and the Yangtze River Delta (Li *et al.*, 2020; Zhang *et al.*, 2023). This led to the implementation in 2013 of a range of policies to try to reduce $O_3$ precursor emissions across China e.g. a comprehensive management plan to control volatile organic compounds (VOCs) from key industries, an atmospheric pollution prevention and control law of the People's Republic of China and the 2020 VOCs Management Plan (Li, Zhou and Xu, 2021). As a result, nitrogen oxide (NOx) emissions, an important $O_3$ precursor, have decreased significantly from 2013 to 2017 by 21% (Li, Zhou and Xu, 2021). By contrast, VOCs have only slightly decreased by 2% over the same time period. Since China has a VOC limited O3 regime the reductions in NOx lead to rather insignificant changes in $O_3$ concentration (Li, Zhou and Xu, 2021) though evidence suggests that reductions in $O_3$ may be higher in rural than urban areas (Lee *et al.*, 2020). This implies future policies to tackle ground level $O_3$ pollution in China need to increase their focus on reducing VOCs along with NOx (Lee *et al.*, 2020).

At present, methods to assess the risk to crop productivity from changes in $O_3$ and climate variables have used a variety of different $O_3$ risk assessment methods. Such methods in the past relied heavily on dose-response relationships, empirically derived relationships that assess changes in a response variable (most commonly yield) against an ozone exposure metric (concentration or, more recently flux-based indices). By contrast, methods to assess the impact of climate variables (most commonly changes in temperature, precipitation, and $CO_2$ concentration) tend to use crop models since these allow the integration of the combined effect of a number of different variables acting simultaneously to affect crop development, growth, and yield (Schauberger *et al.*, 2019). There has been a growing awareness of the need to integrate the ozone effect within crop models so that a holistic assessment of the combined impacts resulting from these stressors can be achieved (Tao *et al.*, 2017; Emberson *et al.*, 2018; Schauberger *et al.*, 2019).

The $DO_3SE$ model is an ozone deposition model that can be embedded within atmospheric chemistry transport models (e.g. Simpson et al., 2012) and uses either a multiplicative- or coupled $A_{net}$-$g_{sto}$ model to estimate stomatal ozone flux (Pande et al., sub). Accumulated stomatal ozone flux has been successfully used as a damage metric (PODy - Phytotoxic Ozone Dose over a threshold y (LRTAP, 2017)) to predict ozone-induced yield loss (Pande et al., sub). The ability of the $DO_3SE$ model to simulate $A_{net}$, and the inclusion of a process-based ozone damage module for both instantaneous $A_{net}$ and early and enhanced senescence (after (Ewert and Porter, 2000)) lends itself to the development of the $DO_3SE$ model as a process-based crop model. The inclusion of resistance algorithms that can assess the transport of $O_3$ concentrations from a reference height above a canopy down to the canopy top, mean the model can easily be embedded within existing atmospheric chemistry transport schemes and hence applied for regional or global scale $O_3$risk

https://doi.org/10.5194/egusphere-2024-694
Preprint. Discussion started: 16 April 2024


assessment whilst also accurately modelling $O_3$deposition. A comparison of the coupled stomatal conductance-photosynthesis ($A_{net}$-$g_{sto}$) model with the multiplicative $g_{sto}$ model within the DO3SE framework has been made in Pande et al. (sub) and showed that the $A_{net}$-$g_{sto}$ model performed equally well, if not better, when used to develop ozone dose-response relationships for European wheat. This provides evidence of the suitability of the new photosynthetic based $g_{sto}$ model in $DO_3SE$.

In this study we describe the development of a new '$DO_3SE$-Crop' model which builds on the modified stomatal deposition component of the $DO_3SE$ model (Pande et al. (sub)) so that both $CO_2$ uptake for carbon assimilation as well as ozone uptake via the stomata can be modelled consistently. Further, we have incorporated the UK JULES crop model (Osborne *et al.*, 2015)to allocate assimilated carbon to plant components (roots, leaves, stems and harvest organs) according to crop development stage. We also take account of the modifying effect of ozone on instantaneous $A_{net}$ as well as the onset and rate of leaf senescence and timing of crop maturity through incorporation of algorithms developed by (Ewert and Porter, 2000).The UK JULES crop model is used since this is the UK land surface exchange scheme in the UK Earth System Model (UKESM) (Osborne *et al.*, 2015)which has recently been developed to include exchange and impact of trace gases (including $O_3$) along with other biogeochemical cycling between the atmosphere and the land surface (Leung *et al.*, 2020). This would allow comparison of the UK JULES Crop model which are based on (Sitch *et al.*, 2007) with the alternative $O_3$ damage mechanisms used within $DO_3SE$-crop.

Here we calibrate and evaluate $DO_3SE$-crop model using an experimental FACE dataset collected in Xiaoji, China. This allows us to investigate the ability of the model to simulate $O_3$ damage for a global region where crop productivity is severely threatened by both ozone pollution and climate change. The key objectives of the paper are to: i). assess the ability of $DO_3SE$-Crop to simulate key physiological variables, crop development, biomass and yield; ii). the ability of DO3SE-crop to estimate the difference in $O_3$ induced yield loss for tolerant and sensitive cultivars caused due to instantaneous versus long-term senescence effects on photosynthesis, and iii). the applicability of the prescribed UK JULES crop parameters for Chinese conditions.

https://doi.org/10.5194/egusphere-2024-694
Preprint. Discussion started: 16 April 2024


## Methods : $DO_3SE$-Crop Model development, calibration and Evaluation

### 1. $DO_3SE$-Crop Model

We describe the development and calibration of '$DO_3SE$-Crop' (version 4 (V4.39.19)), an ozone deposition model (Emberson *et al.*, 2000; Simpson *et al.*, 2012)that has been modified to simulate stomatal conductance from a coupled photosynthesis-stomatal conductance model (Leuning, 1995). Photosynthesis is simulated using a biochemical model (Farquhar, Caemmerer and Berry, 1980; Sharkey *et al.*, 2007). The $DO_3SE$ model has also been extended to include a photosynthetic-based crop model based on the UK JULES land surface crop model (Osborne *et al.*, 2015) with ozone damage functions incorporated after (Ewert and Porter, 2000). $DO_3SE$-Crop is designed to simulate ozone deposition and stomatal uptake and the effects of ozone and climate related variables on crop development, biomass and yield. The DO3SE-Crop model has been developed to simulate wheat (*Triticum aestivum*) which is widely considered to be one of the most sensitive staple crops to ozone (Feng *et al.*, 2018).

The key components of $DO_3SE$ Crop are illustrated in Fig.1 and can be defined as i). crop phenology to ensure the correct length and timing of crop growth for carbon assimilation and ozone exposure; ii). leaf scale processes to ensure leaf level estimates of photosynthesis and stomatal conductance for sunlit and shaded leaves are able to accurately model carbon assimilation and stomatal ozone flux and associated damage over the leaf life span; iii). leaf-to-canopy upscaling that incorporates a within canopy irradiance and ozone concentration gradient and iv). carbon allocation processes to ensure carbon is allocated correctly to different crop compartments (roots, leaves, stem, grain) throughout the growing season.

Fig. 1 Schematic of $DO_3SE$-Crop

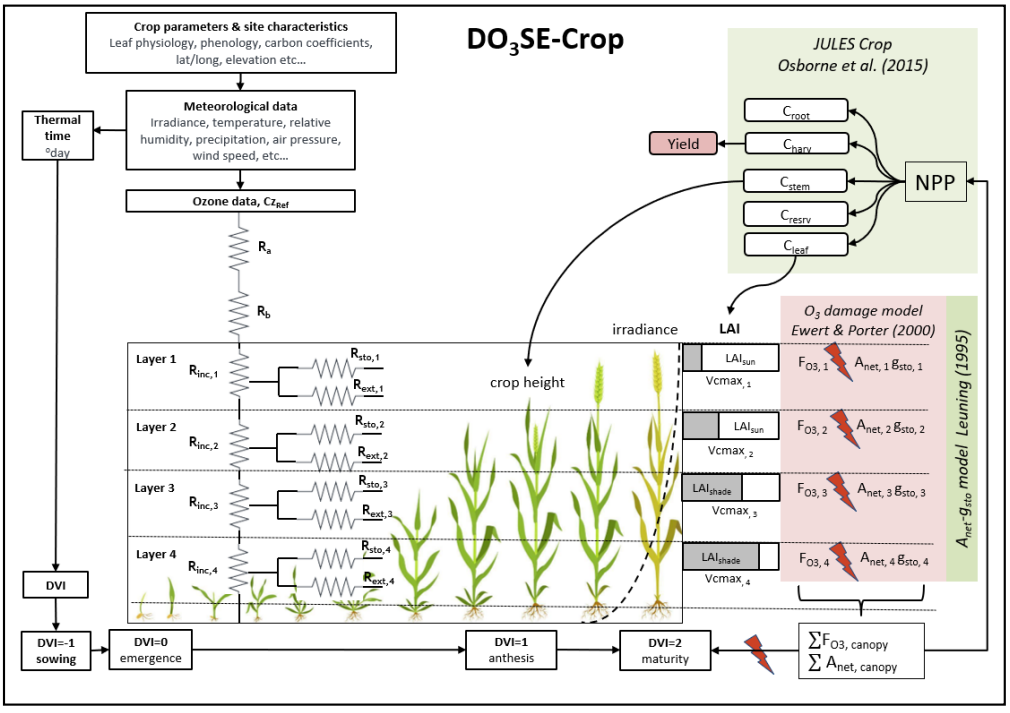

https://doi.org/10.5194/egusphere-2024-694
Preprint. Discussion started: 16 April 2024


### 1.1 DO$_3$SE Crop Phenology

The DO$_3$SE-Crop model uses thermal time ($TT$) to define the rate of crop development in relation to the timing of three key developmental stages, $TT_{emr}$ (the period from sowing to emergence), $TT_{veg}$ (the period of emergence to start of grain filling) and $TT_{rep}$ (the period from the start of grain filling to maturity) based on the method of (Osborne *et al.*, 2015). $TT$ is calculated by estimating an effective temperature ($T_{eff}$) using base ($T_b$), optimum ($T_o$) and maximum ($T_m$) cardinal temperatures.

$$T_{eff} = \begin{cases} 0 & for\ T_{air} < T_b \\ T_{air} - T_b & for\ T_b \leq T_{air} \leq T_0 \\ (T_0 - T_b)\left(1 - \frac{T_{air} - T_0}{T_m - T_0}\right) & for\ T_0 < T_{air} < T_m \\ 0 & for\ T_{air} \geq T_m \end{cases} \quad [1]$$

Where, $T_{air}$ is the surface air temperature in °C, $T_{eff}$ is at a maximum when $T_{air} = T_o$, this point denotes the highest developmental rate. $T_{eff}$ declines as the temperature falls or rises above $T_o$, with a linear decrease in crop development. $T_{eff}$ is zero, i.e. no development, when $T_{air}$ falls below or rises above $T_b$ and $T_m$ respectively i.e., $T_m \leq T_{air} < T_b$. During the sowing to emergence phase, development is dependent on $T_b$, whereas during the vegetative and reproductive phase, development depends on $T_m$ or $T_o$.

Winter wheat requires vernalisation (a period of exposure to low temperature during germination to accelerate flowering). Vernalisation alters the length $TT_{veg}$ and hence flowering initiation, with subsequent effects on later growth stages such as heading. Vernalisation occurs when the minimum ($VT_{min}$) and maximum ($VT_{max}$) daily temperature is less than 15°C and 30°C respectively (Zheng et.al., 2015). Accumulated vernalised days ($V_{dd}$) are calculated as the sum of vernalised and devernalised days from emergence to the start of anthesis (Zheng *et al.*, 2015).

$$V_{dd} = \sum(V - V_d), \text{ where} \quad [2]$$

$$V = \left(1.4 - 0.778 \times T_{air}, 0.5 + 13.44\frac{T_{air}}{(Tmax - Tmin + 3)^2}\right) \text{ for } VT_{max} < 30°C \text{ and } VT_{min} < 15°C$$

$$V_d = (min(0.5(T_{max} - 30), Vprev) \quad \text{for } VT_{max} > 30°C \text{ and } V_{dd} < 10 \text{ days}$$

The vernalisation factor ($VF$) decreases from 1 to 0 as ($V_{dd}$) increases. $VF$ depends on a cultivar-specific vernalisation coefficient ($PIV$) as described by eq. 3.

$$VF = 1 - (0.0054545 \times PIV + 0.0003) * (50 - V_{dd}) \quad [3]$$

Photoperiod ($PP$) or day length also affects the occurrence and timing of the flowering stage and is calculated according to latitude using standard solar geometry to estimate daylength (Jones, 1992). The photoperiod factor ($PF$) represents the sensitivity to $PP$ which decreases from 1 to 0 as the photoperiod shortens and is estimated according to a cultivar-specific photoperiod coefficient ($PID$) after Tao et al. (2012) as described in eq. 4.

$$PF = 1 - \left[\left(\frac{PID}{10000}\right) \times (20 - PP)^2\right] \quad [4]$$

Crop development is related to the development index ($DVI$) after (Osborne *et al.*, 2015) which takes values of -1 upon sowing, 0 on emergence, 1 at anthesis and 2 at crop maturity. The DO$_3$SE-Crop model $DVI$ equations have been modified from (Osborne *et al.*, 2015) to take account of the photoperiod and vernalisation for winter wheat (see eq. 5); for spring wheat these factors are omitted.

https://doi.org/10.5194/egusphere-2024-694
Preprint. Discussion started: 16 April 2024


$$-1 \leq DVI < 0 \qquad for\ td < TT_{emr}$$

$$0 \leq DVI < 1 \qquad for\ TT_{emr} \leq td \times VF \times PF < TT_{veg} \qquad [5]$$

$$1 \leq DVI \leq 2 \qquad for\ TT_{veg} \leq td \leq TT_{rep}$$

$DO_3SE$-Crop allows for any number of representative leaf populations ($pop$) and canopy layers ($n$) to be defined over the course of the crop growing season. In this study, we used a single leaf population and 4 canopy layers (i.e. $pop = 1;\ n = 4$) for simplicity. The crop sowing is assumed to be at DVI = -1 (start of $TT_{emr}$) and emergence at DVI =0 (start of $TT_{veg}$). The flag leaf is assumed to develop at $DVI$=1, at the commencement of TTrep, marking the initiation of anthesis ($A_{start}$ ,flowering) and flag leaf emergence, which typically occurs 4-5 days prior to the onset and is further divided into expanding and senescing leaf periods (i.e. $tl_{ep}$ and $tl_{se}$) with a default ratio of 0.67 to 0.33 Maturity is assumed at DVI =2 end of $TT_{rep}$). The model allows estimation of the $PODy$ metric by accumulating stomatal ozone flux from the start of anthesis to maturity. The total leaf life span ($TT_{leaf}$) of the crop is distributed over the DVI between 0 and 2. The relationship between these different variables are described in Fig. 2).

### 1.2 $DO_3SE$-Crop leaf-level physiology

Key leaf-level physiological variables of the $DO_3SE$-Crop model are net photosynthesis ($A_{net}$) and stomatal conductance ($g_{sto}$). Net photosynthesis is simulated using the biochemical photosynthesis-based model initially developed by (Farquhar, G.D., von Caemmerer, S., Berry, 1980)and since modified by (Sharkey *et al.*, 2007). The coupled $A_{net}g_{sto}$ model of (Leuning, 1995) is used to estimate $g_{sto}$ from $A_{net}$ which means that $g_{sto}$ is regulated by the demand of $CO_2$ for $A_{net}$ on consideration of environmental conditions and crop physiology. Ozone stress, causing both instantaneous effects on $A_{net}$ and long-term effects on leaf senescence, is simulated based on algorithms developed by (Ewert and Porter, 2000).

#### 1.2.1 Leaf net photosynthesis ($A_{net}$)

The $A_{net}$ model assumes that photosynthesis is constrained depending on prevailing environmental conditions according to three main mechanisms: Rubisco activity ($A_c$); ribulose-1,5-bisphosphate (RuBP) regeneration, which is constrained by the speed of electron transport ($A_j$); and the low rate of transfer of photosynthetic products (most frequently triose phosphate consumption) ($A_p$) (Sharkey *et al.*, 2007a) and by soil water stress ($f_{sw}$); the algorithm for $A_c$ which is based on (Medlyn *et al.*, 2002) and modified in DO3SE-crop to include the $O_3$ damage functions is given in eq. 6.

$$A_c = V_{cmax} . f_{sw} . \frac{(C_i - \Gamma^*) \times fO_{3,s}(d) \times f_{LS}}{C_i + K_c\left(1 + \frac{O_i}{K_o}\right)} \qquad [6]$$

where $Vc_{max}$ (µmol $CO_2$ $m^{-2}s^{-1}$) is the maximum carboxylation capacity at 25°C, $C_i$ (µmol $mol^{-1}$) and $O_i$ (mmol $mol^{-1}$) are the intercellular $CO_2$ and $O_2$ partial pressures; $K_c$ (µmol $mol^{-1}$) and $K_0$ (mmol $mol^{-1}$) are the Rubisco Michaelis-Menten constants for $CO_2$ and $O_2$; $\Gamma^*$ (µmol $mol^{-1}$) is the $CO_2$ compensation point in the absence of respiration; $fO_{3,s}(d)$ is the factor that accounts for the cumulative stomatal $O_3$ flux effect on $V_{cmax}$ over the course of a day and; $f_{LS}$ is the factor that accounts for the cumulative stomatal $O_3$ flux effect over the course of a leaf life span on leaf senescence. Section 1.2.1.1 gives a full description of the methods used to estimate $O_3$ damage. The $f_{PAW}$ factor is calculated by eq. 7.

$$f_{PAW} = min\{1, max\{f_{min},\ f_{min} + (1 - f_{min}) \times \frac{(ASW / ASW_{fc}) \times 100 - ASW_{min}}{ASW_{max} - ASW_{min}}\}$$

https://doi.org/10.5194/egusphere-2024-694
Preprint. Discussion started: 16 April 2024


Where: $f_{PAW}$ is the plant available water factor, influencing stomatal conductance. $f_{min}$ is the minimum stomatal conductance under dry soil conditions. ASW represents the available soil water. $ASW_{fc}$ is the available soil water at field capacity, converted to a percentage. $ASW_{max}$ is the plant available soil water below which stomatal conductance will start to reduce, and $ASW_{min}$ is the plant available soil water at which stomatal conductance will equal $f_{min}$ (Nguyen *et al.*, 2024).

This model scales the stomatal conductance between a minimum value and a value of unity, which represents fully open stomata, based on the available soil water as a percentage of its field capacity. The constraint on $A_{net}$ due to the rate of electron transport $A_j$ is described in eq. [8].

$$A_j = J \times \frac{C_i - \Gamma^*}{a \times C_i + b \times \Gamma^*} \quad [8]$$

where $J$ is the electron transport rate (µmol $CO_2$ $m^{-2}s^{-1}$), the parameters $a$ and $b$ denote the electron requirements for the formation of NADPH and ATP respectively (Sharkey *et al.*, 2007)

Finally, the $A_{net}$ limitation due to the low rate of transfer of photosynthetic products $A_p$(µmol $CO_2$ $m^{-2}s^{-1}$) is given in eq. [9].

$$A_p = 0.5 \times V_{cmax} \quad [9]$$

The net leaf photosynthetic carbon uptake ($A_{net}$) in µmol $CO_2$ $m^{-2}s^{-1}$ is calculated by eq. [10]

$$A_{net} = (A_c, A_j, A_p) - R_d \quad [10]$$

Where leaf dark respiration ($R_d$) in µmol $CO_2$ $m^{-2}s^{-1}$ is calculated as $Vc_{max} \times R_{dcoeff}$ where $R_{dcoeff}$ is the leaf dark respiration coefficient initially set equal to 0.015 after Clark et al. (2011), a value provided for C3 grasses.

#### 1.2.1.1 Short- and long-term $O_3$ damage to $A_c$

The short-term impact of $O_3$ on $A_c$ is calculated according to the $fO_{3,s}(d)$ factor (between 0 and 1) which allows for an instantaneous effect of $O_3$ on photosynthesis when stomatal $O_3$ flux ($f_{st}$), in nmol $O_3$ $m^{-2}$ $s^{-1}$ calculated as described later in section 1.2.3, overwhelms detoxification and repair mechanisms (Betzelberger *et al.*, 2012; Feng *et al.*, 2022), and is estimated following (Ewert and Porter, 2000). Here, $f_{O3,s}(h)$ represents the relationship between $f_{st}$ and a potential decrease in $A_c$ calculated for every hour by eq. [11].

$$f_{O3,s}(h) = 1\,; \qquad for\ f_{st} \le \frac{\gamma 1}{\gamma 2}$$

$$f_{O3,s}(h) = 1 + \gamma 1 - \gamma 2 \times f_{st} \qquad for\ \frac{\gamma 1}{\gamma 2} < f_{st} < \frac{1+\gamma 1}{\gamma 2} \quad [11]$$

$$f_{O3,s}(h) = 0\,; \qquad for\ f_{st} \ge \frac{1+\gamma 1}{\gamma 2}$$

where $\gamma 1$ (dimensionless) and $\gamma 2$ (nmol $O_3$ $m^{-2}$ $s^{-1}$)$^{-1}$ are both short-term $O_3$ damage coefficients, with $\gamma 1$ representing the $O_3$ detoxification threshold below which no damage occurs to the photosynthetic system and $\gamma 2$ determines the effect of $f_{st}$ on $A_c$ once this detoxification threshold is exceeded; $fO_{3,s}(d)$ and $fO_{3,s}(d-1)$ i.e. $fO_{3,s}(d)$ at the end of the previous day, are calculated by eq. [12].

$$f_{O3,s}(d) = f_{O3,s}(h) \times r_{O3,s} \qquad for\ hour = 0;$$

$$f_{O3,s}(d) = f_{O3,s}(h) \times f_{O3,s}(d-1) \qquad for\ hour = 0 \quad [12]$$

https://doi.org/10.5194/egusphere-2024-694
Preprint. Discussion started: 16 April 2024


where $r_{O3,s}$ (dimensionless) is incomplete recovery from $O_3$ overnight which depends on leaf age according to eq. [13].

$$r_{O3,s} = f_{O3,s}(d-1) + \left(1 - f_{O3,s}(d-1)\right) \times f_{LA} \quad [13]$$

The long-term impact of $O_3$ on $V_{cmax}$ represented by the $f_{Ls}$ term represents the longer-term accumulation of stomatal ozone flux ($acc_{fst}$) causing degradation to the Rubisco enzyme which triggers early and enhanced senescence of mature leaves (Gelang *et al.*, 2000; Osborne *et al.*, 2019). The simulation of $f_{Ls}$ (and $f_{LA}$ used in the short-term $O_3$ effect) are related to thermal time defined periods over the course of a leaf life span $TT_{leaf}$ as described in Fig. 2.

Figure 2. The division of thermal time defined periods ($TT_{emr}$ , $TT_{veg}$, $TT_{rep}$ and $TT_{leaf}$ and the relationship with $f_{LA}$ and $f_{Ls}$).

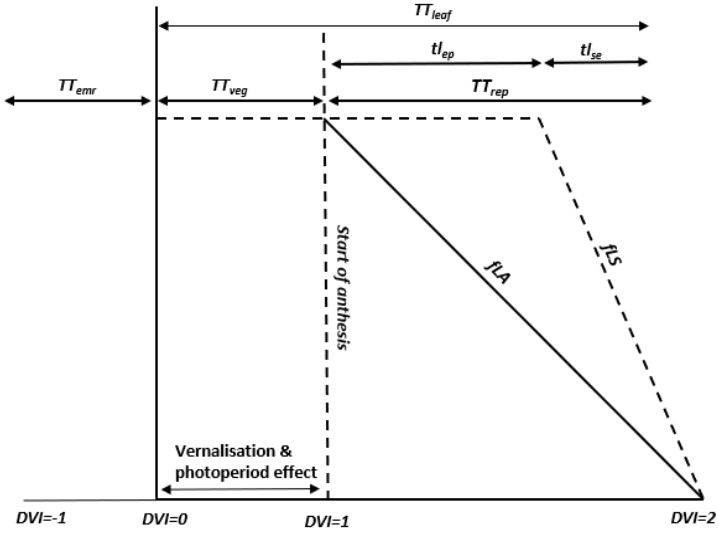


The $O_3$ effect on $f_{Ls}$ is first simulated by estimating a weighted accumulated $fst$ ($fO3_l$) modified from (Ewert and Porter, 2000)by eq. [14].

$$fO3_l = 1 - max(min\left(\gamma 3 \times \left(acc_{fst} - CLsO3\right), 1\right), 0) \quad [14]$$

where $\gamma 3$ determines the occurrence of senescence once a critical cumulative stomatal $O_3$ flux $CLsO3$ (in mmol/m$^2$) has been exceeded. The rate of senescence is determined by $\gamma 4$, which determines the onset of senescence and $\gamma 5$ which determines maturity as described in eq. [15]

$$tl_{ep_{O3}} = tl_{ep} \times (1 - \left((1 - fO3_l) \times \gamma 4\right))$$

$$tl_{se_{O3}} = tl_{se} \times \left(1 - \left((1 - fO3_l) \times \gamma 5\right)\right) + zc \quad [15]$$

$$zc = tl_{ep} - tl_{ep_{O3}}$$

Where $tl_{ep}$ is the effective temperature ($teff$) accumulated by a leaf in °C days between a fully expanded leaf and the start of leaf senescence, $tl_{ep_{O3}}$ is $tl_{ep}$ with an $O_3$ effect which may bring

https://doi.org/10.5194/egusphere-2024-694
Preprint. Discussion started: 16 April 2024


senescence earlier, $tl_{se}$ is the $(teff)$ between the onset of senescence and maturity and $tl_{se_{O3}}$ is $tl_{se}$ with an $O_3$ effect which may bring maturity earlier. $f_{Ls}$ is estimated by eq. [16].

$$f_{Ls} = 1; \qquad for\ \ teff \leq TT_{veg} + tl_{ep}$$

$$f_{Ls} = 1 - \frac{TT_{eff} - TT_{veg} - tl_{ep_{O3}}}{tl_{se_{O3}}}; \qquad for\ TT_{veg} + tl, ep < teff < TT_{leaf}$$

$$f_{Ls} = 0; \qquad for\ teff \geq TT_{leaf} \qquad [16]$$

### 1.2.2 Stomatal conductance

The coupled photosynthesis-stomatal conductance ($A_{net} g_{sto}$) model based on (Leuning, 1995) and modified for vapour pressure deficit ($VPD$) is used to estimate $g_{CO_2}$, stomatal conductance to $CO_2$ in µmol $CO_2$ $m^{-2}$ $s^{-1}$ as described in eq. [17].

$$g_{CO2} = [f_{min} + m \times A_{net} \times f_{VPD}/(c_s - \Gamma)] \qquad [17]$$

where $f_{min}$ (µmol $m^{-2}$ $s^{-1}$) is the minimum daytime $g_{CO_2}$ (Leuning, 1990). The parameter $m$ (dimensionless) is the composite sensitivity of $g_{CO2}$ to assimilation rate and vapour pressure deficit ($VPD$) with the relationship between $VPD$ and relative stomatal conductance ($f_{VPD}$) estimated by eq. [18]. $A_{net}$ (µmol m-2 s-1) is estimated from eq [10]. $f_{VPD}$ is calculated by eq. [18].

$$f_{VPD} = \left(1 + \left(\frac{VPD}{VPDo}\right)^8\right)^{-1} \qquad [18]$$

where $VPD_0$ is an empirical parameter, defined using boundary line analysis, describing the variation in relative stomatal conductance with $VPD$ (Danielsson *et al.*, 2003; Pleijel *et al.*, 2007). $c_s$ (mmol $mol^{-1}$) is the external $CO_2$ concentration at the leaf surface and is calculated from the external $CO_2$ concentration at the upper surface of the leaf boundary layer $c_a$ (mmol $mol^{-1}$) so that $c_s = c_a - \left(\frac{A_{net}}{g_{bCO2}}\right)$ after (Masutomi, 2023) where $g_{bCO2}$ is the boundary layer conductance to $CO_2$ (in mol $m^{-2}$ $s^{-1}$), conversion factors for the boundary layer are given in S1a.

Finally, $g_{CO2}$ is converted to $g_{O3}$ in mmol $O_3$ $m^{-2}$ $s^{-1}$ by dividing by 1000 and using the conversion factor 0.96 which assumes that the ratio of the diffusivities of gases in air are equal to the inverse of the square root of the ratio of molecular weights (as described in (Campbell, G.S., Norman, 1998), see also supplementary S1).

### 1.2.3 Stomatal ozone flux ($f_{st}$)

Stomatal [$O_3$] flux $f_{st}$ (nmol $m^{-2}$ $s^{-1}$) is calculated after the method described in the UNECE Mapping Manual (UNECE, 2017) described in eq. [19].

$$f_{st} = C_l \times\ g_{O3m/s} \times \frac{r_c}{r_{b,O3} + r_c} \qquad [19]$$

Where $C_l$ is the [$O_3$] at the upper surface of the laminar layer of a leaf (nmol $O_3$ $m^{-3}$). Ozone concentration in ppb can be converted to nmol $m^{-3}$ by multiplying $O_3$ in ppb by $P/(R \times T_{air,k})$ where $P$ is the atmospheric pressure in Pascal, $R$ is the universal gas constant (8.31447 J/mol/K) and $T_{air,k}$ is surface air temperature in degrees Kelvin; $g_{O3m/s}$ (m/s) is stomatal conductance to $O_3$, to convert $g_{O3}$ (mol $O_3$ $m^{-2}$ $s^{-1}$) to $g_{O3m/s}$ (m/s) we assume a standard temperature $T_{st}$(20°C) and air pressure $P_{st}$ ($1.013 \times 10^5$ in Pascal) and divide by 41 to give the conductance value in m/s. The $r_c/r_{b,O3}+r_c$ term represents the $O_3$ deposition rate to the leaf through resistances $r_b$ (the quasi-laminar resistance (s/m)) and $r_c$ (the leaf surface resistance (s/m)) which allow for both stomatal and

https://doi.org/10.5194/egusphere-2024-694
Preprint. Discussion started: 16 April 2024


non-stomatal deposition to the leaf surface. $r_c$ is 1/($g_{O3m/s}$+$g_{ext}$) where $g_{ext}$ is 1/2500 (s/m). $r_b$ is estimated by eq. [20].

$$r_{b,O3} = 1.3 \times 150 \times \sqrt{\frac{L}{u_l}} \quad [20]$$

Where the factor 1.3 accounts of the differences in diffusivity between heat and $O_3$. and The value of 150 provides the equivalent conductance leaf layer for $O_3$ as compared to forced convection of heat (Campbell, G.S., Norman, 1998), $L$ is the cross wind leaf dimension (m) and $u_l$is the windspeed (m/s) at the top of the leaf laminar boundary layer. The leaf boundary layer resistance to $CO_2$ is estimated using a value of 1.24 for the difference between heat and $CO_2$ in place of the 1.3 value for $O_3$ (Campbell, G.S., Norman, 1998).

### 1.3 DO$_3$SE-Crop canopy

The DO$_3$SE crop model uses a multi-layer approach to scale from leaf to the canopy. We assume that wind, irradiance, [$O_3$] concentration and leaf nitrogen content are the key environmental conditions which change with cumulative canopy leaf area index ($LAI$) and influence leaf physiology and therefore canopy layer estimates of $A_{net}$, $g_{sto}$ and $g_{ext}$; other environmental variables (e.g., $T_{air,oC}$ and $VPD$) are assumed to remain constant over the canopy.

#### 1.3.1 Canopy irradiance

Changes in irradiance through the canopy are described as sunlit and shaded canopy fractions and the associated quantity of direct and diffuse photosynthetically active radiation $PAR$ (W/m$^2$), these are estimated according to increasing levels of cumulative $LAI$ using the methods of (Pury and Farquhar, 1997); full details are given in the supplementary material (see section S2). Application of this method requires the canopy to be divided into layers of equal $LAI$ (including both green ($LAI_G$) and brown ($LAI_B$) $LAI$.

$PAR$ absorbed per unit leaf area is divided into $PAR_{dir}$, $PAR_{diff}$ which also includes scattered (re-reflected by the canopy) beam calculated by,

$$PAR_{dir}\ (LAI) = (1 - \rho_{cb}(\beta))\ K_b'\ I_b(0)\ exp(-k_b\ 'LAI) \quad [21]$$

$$PAR_{diff}\ (LAI) = \ (1 - \rho_{cd})\ K_d'\ I_d(0)\ exp(-k_d'LAI) \quad [22]$$

Estimates of the $LAI$ fractions of sunlit ($LAI_{sun}$) and shaded ($LAI_{sh}$) parts of each canopy layer ($i$) are made by eq. 23 and 24.

$$LAI_{sun,i} = \left[1 - exp\ \left(-0.5 \times \frac{LAIi}{sin\beta}\right)\right] \times 2sin\beta \quad [23]$$

Where $\beta$ is the solar elevation angle (see supplementary section S3)

$$LAI_{sh,i}\ =\ LAI_i - LAI_{sun,i} \quad [24]$$

The DO$_3$SE-Crop model simulates $LAI$ as part of the crop growth model and LAI is assumed to be evenly distributed across all layers (see section 1.5.2 and eq. 43).

Therefore, PAR for the sunlit part of each layer can be described as

$$\int_{LAI_i}^{LAI_n} PA\,R_{sun} = \int_{LAI_i}^{LAI_n} (\,LAI_{sun,i}) \times (PAR_{sh} + PAR_{bsun}\ (\beta))\ \text{dLAI}$$

https://doi.org/10.5194/egusphere-2024-694
Preprint. Discussion started: 16 April 2024


Where $\int_{LAi_i}^{LAi_n} P\,AR_{dir}$ can be written as $(1-\rho cb(\beta)) \times Kb' \times Ib(0) \times [exp(-Kb'LAI_i) - exp(-Kb'LAI_n)]$ and $PAR_{bsun}\,(\beta) = (1-\sigma)I_b(0)\frac{Cos_{\alpha l}}{Sin\beta}$

Similarly; PAR for the shaded part of each layer can be described as

$$\int_{LAI_i}^{LAI_n} PA\,R_{sh} = \int_{LAI_i}^{LAI_n} (LAI_{sh,i}) \times (PAR_{diff} + PAR_{bs})dL\text{AI}$$

Where $\int_{LAi_i}^{LAi_n} (PAR_{diff}\,(LAI)$ can be written as $(1-\rho cd) \times Kb' \times Ib(0) \times [exp(-k_d{}'LAI_i) - exp(-k_d{}'LAI_n)]dL$ and $\int_{LAi_i}^{LAi_n} P\,AR_{bs}\,(LAI)$ is $I_b\,(0)\,[\,PAR_{dir} - (1-\sigma)k_b \times [exp(-k_bLAI_i) - exp(-k_bLAI_n)]$

### 1.3.2 Canopy [$O_3$] concentration

$O_3$ concentration will vary as a function of $O_3$ loss to the canopy (i.e. deposition via the stomates and external plant parts) and $O_3$ replacement from ambient air concentrations above the canopy. Limited data have been collected showing how $O_3$ concentrations vary with canopy depth in semi-natural communities (Jaggi *et al.*, 2006). These data suggest that a minimum, bottom canopy $O_3$ concentration ($c_{zb}$), is about 0.2 times that at the top of the canopy ($c_{zh}$) and that the $O_3$ concentration difference within the canopy is closely related to the $LAI$ of the canopy layers.

Since each canopy layer can be assumed to be a parallel sink, the $O_3$ flux to a layer depends on the conductance (inverse of resistance) of that layer and the $O_3$ concentration at the top of the layer ($C_i$; with $C_0$ being $c_{zh}$ (i.e. the $O_3$ concentration at height $C_h$, the top of the canopy)); we follow and generalise the work of Waggoner.,1971 by separating the canopy into $nL$ leaf layers. We calculate the $O_3$ concentration for each layer, $C_i$, from $O_3$ intake, $I_i$, by;

$$C_i = r_i I_i \qquad [25]$$

With $r_i$ the surface resistance for layer $i$. $I_i$ is calculated as the solution to a system of linear equations. Relating $r_i$, $I_i$, and $R_i$, the in-canopy aerodynamic resistance for layer $i$. Assuming above the canopy there is a uniform $O_3$ concentration $C_0$, we use generalised equations from Waggoner., 1971 for the difference in $O_3$ concentration between the exterior air and leaf interior, which for the top layer is $C_0$ minus 0, so $C_0$ and for each lower layer the difference is 0. This $O_3$ concentration difference is calculated by;

$$C_0 = R_1 \sum_{j=1}^{nL} I_j + r_1 I_1 \qquad [26]$$

For the top canopy layer,

$$0 = R_i \sum_{j=i}^{nL} I_j + r_i I_i - r_{i-1} I_{i-1} \qquad [27]$$

For each canopy layer $i$ between the top layer and the bottom layer, and;

$$0 = R_{nL+1} I_{nL+1} - r_{nL} I_{nL} \qquad [28]$$

For the bottom layer of the canopy, between the lowest leaf layer and the ground. These can also be written into the matrix form;

$$\begin{pmatrix} r_1 + R_1 & R_1 & R_1 & \cdots & R_1 \\ -r_1 & r_2 + R_2 & R_2 & \cdots & R_2 \\ 0 & -r_2 & r_3 + R_3 & \cdots & R_3 \\ \vdots & \vdots & \vdots & \ddots & \vdots \\ 0 & 0 & 0 & \dots & R_{nL+\_1} \end{pmatrix} \begin{pmatrix} I_1 \\ I_2 \\ I_3 \\ \vdots \\ I_{nL+1} \end{pmatrix} = \begin{pmatrix} C_0 \\ 0 \\ 0 \\ \vdots \\ 0 \end{pmatrix} \qquad [29]$$

https://doi.org/10.5194/egusphere-2024-694
Preprint. Discussion started: 16 April 2024


Which can be numerically solved for $I_x$ when $r_1 \neq 0$ and $R_1 \neq 0$.

Resistances for each layer are calculated as described in the supplementary material (section S4) using standard DO$_3$SE deposition modelling methods (Emberson, L.D., Ashmore, M.R., Simpson, D., Tuovinen, J.-P. and Cambridge, 2001; Simpson *et al.*, 2012).

### 1.3.3 Canopy maximum carboxylation capacity ($V_{cmax}$)

We allow for an exponential decrease in leaf N with canopy depth which will influence both the photosynthetic capacity ($V_{cmax}$) and hence dark respiration ($R_d$). Photosynthetic capacity at each canopy layer $i$ is calculated by eq. [30].

$$V_{cmax,i} = n_e \times n_0 \times e^{-kN\left(\frac{LAIi}{LAItotal}\right)} \quad [30]$$

Where $n_e$ (mol CO$_2$ m$^{-2}$ s$^{-1}$ kg C (kg N)$^{-1)}$ is a constant relating leaf nitrogen to Rubisco carboxylation capacity, $n_0$ (kg N[kg C]-1) is the leaf N concentration at the top of the canopy and $kN$ is a nitrogen profile co-efficient initially set at 0.78 after (Clark *et al.*, 2011).

### 1.3.4 Canopy Photosynthesis ($Anet_c$)

Net canopy photosynthesis ($Anet_c$) determines the amount of C assimilated by the entire canopy that can subsequently be allocated to different plant parts (i.e. less than the C respired for plant growth and maintenance, see section 1.4.1), the amount of C assimilation will ultimately determine whole plant biomass. The net photosynthesis for each canopy layer ($Anet_i$) is calculated according to the $LAI$ fraction of that layer that is sunlit ($LAI_{sun,i}$) and shaded ($LAI_{sh,i}$) within the layer ($i$), multiplied by the net photosynthesis of the sunlit ($Anet_{sun,i,j}$) and shaded leaf ($Anet_{sh,i,j}$), respectively described by eq. [31] and [32].

$$Anet_i = LAI_{sun,i} \times Anet_{sun,i} + LAI_{sh,i} \times Anet_{sh,i} \quad [31]$$

with $Anet_c$ calculated by,

$$Anet_c = \sum_{i=1}^{n} Anet_i \quad [32]$$

$Anet_c$ is converted from µmol CO$_2$ m$^{-2}$ s$^{-1}$ to kg C m$^{-2}$ day$^{-1}$ by multiplying by 3600 (converting from seconds to hours), multiplying by 1.2 (representing the kg of C per mol) and summing each hourly $Anet_c$ over the course of a day. This $Anet_c$ is used in the equation 37.

### *1.3.5 Canopy Stomatal Conductance* ($g_{sto_i}$)

Similarly, canopy layer ($i$) stomatal conductance to O$_3$ ($g_{O3_i}$) , which is converted from $g_{CO_2}$ by assuming a diffusivity ratio of 0.96 to convert from CO$_2$ to O$_3$ and is calculated by eq. [33] with whole canopy stomatal conductance calculated by eq. [34].

$$g_{sto_i} = LAI_{sun,i} \times g_{sto_{sun,i}} + LAI_{sh,i} \times g_{sto_{sh,i}} \quad [33]$$

$$g_{sto_c} = \sum_{i=1}^{n} g_{sto_i} \quad [34]$$

This is converted from $g_{sto_i}$ in eq. [33] by dividing the conductance value in mmol m$^{-1}$ s$^{-1}$ by 41000 (assuming standard temperature (20°C) and air pressure (1.013 x 10$^5$ Pa)) to give conductance in m/s.

### 1.4 Crop biomass, LAI, height and yield variables

The following section describes how to estimate crop biomass, important canopy characteristics ($LAI$ and crop height ($h$)) and yield variables from accumulated calculations of $Anet_c$ over the course of the growing season following (Osborne *et al.*, 2015).

https://doi.org/10.5194/egusphere-2024-694
Preprint. Discussion started: 16 April 2024


### 1.4.1 Crop biomass ($NPP$ and $GPP$)

The simulation of crop growth requires an estimate of the net primary productivity ($NPP$) which is calculated at the end of each day and summed over the growing season. Carbon is assumed to be allocated to five key crop components: root, leaf, stem, harvest, and reserve pools (Osborne *et al.*, 2015). This carbon allocation is ultimately used to simulate leaf area index ($LAI$), canopy height ($h$), biomass, harvest index, and yield at the end of each day throughout the growing season.

Net primary productivity $NPP$ (kg C m$^{-2}$ day$^{-1}$) is accumulated throughout the day using the JULES-crop approach to model crop growth (Osborne *et al.*, 2015) described in eq. [35].

$$NPP = GPP - R_p \quad [35]$$

where $GPP$ is the gross primary productivity (kg C m$^{-2}$ day$^{-1}$) and $R_p$ is plant respiration divided into maintenance ($R_{pm}$) and growth ($R_{pg}$) respiration (kg C m$^{-2}$ day$^{-1}$) (Clark *et al.*, 2011) where $R_p = R_{pm} + R_{pg}$ and where $R_{pg}$ is assumed to be a fixed fraction of the $NPP$ as shown in eq. [36].

$$R_{pg} = R_{gcoeff}\ (GPP - R_{pm}) \quad [36]$$

Where $R_{gcoeff}$ is the growth respiration co-efficient which was initially set to 0.25 based on the value for all PFTs (i.e. forests and grasses including crops) in (Clark *et al.*, 2011). $GPP$ is calculated by eq. [37].

$$GPP = Anet_c + f_{sw}R_{dc} \quad [37]$$

where $Anet_c$ is net canopy photosynthesis (see eq. 28) and $f_{sw}R_{dc}$ is the soil-moisture modified canopy dark respiration (kg C m$^{-2}$ day$^{-1}$) where $R_{dc} = V_{cmax,i} \times R_{dcoeff}$ with $R_{dcoeff}$ initially assumed to be 0.015 based on (Clark *et al.*, 2011); $V_{cmax,i}$ is the maximum carboxylation efficiency for each canopy layer $i$ which decreases from the top to bottom of the canopy (see eq. 30 ) and $f_{sw}$ is calculated in eq. [7].

Leaf maintenance respiration ($R_{pm}$) is assumed equivalent to the soil moisture modified canopy dark respiration, while root and stem respiration are assumed to be independent of soil moisture but to have the same dependencies on C content. We assume a fixed relationship between C and N contents of these organs so that $R_{pm}$ can be estimated by eq. [38].

$$R_{pm} = R_{dc} \times (f_{sw} + (\frac{C_{root} + C_{stem}}{C_{leaf}})] \quad [38]$$

The C accumulating as $NPP$ each day is divided into five carbon pools i.e. root ($C_{root}$), leaf ($C_{leaf}$), stem ($C_{stem}$), reserve ($C_{resv}$), and harvest ($C_{harv}$) (kg C m$^{-2}$ day$^{-1}$) according to partition coefficients (see eq. [39]) allowing for accumulation of C in these pools over the course of the crop growth period.

$$\begin{aligned} \frac{dC\_root}{dt} &= p_{root}NPP, \\ \frac{dC\_leaf}{dt} &= p_{leaf}NPP, \\ \frac{dC\_stem}{dt} &= p_{stem}NPP\,(1-\tau), \\ \frac{dC\_harv}{dt} &= p_{harv}NPP, \\ \frac{dC_{resv}}{dt} &= p_{stem}NPP, \tau \end{aligned} \quad [39]$$

where $\tau$ is the fraction of stem C that is partitioned into the reserve pool. $p_{root}$, $p_{leaf}$, $p_{stem}$, $p_{harv} = 1$. The partition coefficients are related to the crop development stage ($DVI$) and hence effective thermal time ($TT_{eff}$) since emergence. The partition coefficients are based on Osborne et al. (2015) and provided as a function of $DVI$ using six parameters to continuously describe varying

https://doi.org/10.5194/egusphere-2024-694
Preprint. Discussion started: 16 April 2024


partition coefficients over the duration of the crop growing season. We use the same multinomial logistic as that described in (Osborne *et al.*, 2015) to define this function according to eq. [40].

$$p_{root} = \frac{e^{\alpha_{root}+(\beta_{root}\,DVI)}}{e^{\alpha_{root}+(\beta_{root}\,DVI)} + e^{\alpha_{stem}+(\beta_{stem}\,DVI)} + e^{\alpha_{leaf}+(\beta_{leaf}\,DVI)} + 1},$$

$$p_{stem} = \frac{e^{\alpha_{stem}+(\beta_{stem}\,DVI)}}{e^{\alpha_{root}+(\beta_{root}\,DVI)} + e^{\alpha_{stem}+(\beta_{stem}\,DVI)} + e^{\alpha_{leaf}+(\beta_{leaf}\,DVI)} + 1},$$

$$p_{leaf} = \frac{e^{\alpha_{leaf}+(\beta_{leaf}\,DVI)}}{e^{\alpha_{root}+(\beta_{root}\,DVI)} + e^{\alpha_{stem}+(\beta_{stem}\,DVI)} + e^{\alpha_{leaf}+(\beta_{leaf}\,DVI)} + 1}, \qquad [40]$$

$$p_{harv} = \frac{1}{e^{\alpha_{root}+(\beta_{root}\,DVI)} + e^{\alpha_{stem}+(\beta_{stem}\,DVI)} + e^{\alpha_{leaf}+(\beta_{leaf}\,DVI)} + 1},$$

Where $DVI$ is the development index; $\alpha$ and $\beta$ partition parameters. These parameters describe the shape of the thermal time varying partition coefficient for leaves, roots and stems.

Once C is no longer partitioned to stems, C from the stem reserve pool will mobilise to the harvest pool at a rate of 10% per day following (Osborne *et al.*, 2015) described by eq. [41].

$$C_{harv} = C_{harv} + (0.1\,C_{resv})\,C_{resv} = 0.9\,C_{resv}\,\} \qquad for\ p_{stem} < 0.01 \qquad [41]$$

Total leaf C is divided between green leaf C ($C_{leaf,green}$), and brown leaf carbon ($C_{leaf,brown}$). Carbon from the $C_{leaf,green}$ will mobilise to the harvest pool at the rate of 5% per day after (Osborne *et al.*, 2015) and to the $C_{leaf,brown}$ at a rate of 24% per day once $f_{LS} > 1$ as described in eq. [42]

$$\{C_{harv} = C_{harv} + (0.05\,C_{leaf,green})\,C_{leaf,green} = 0.86\,C_{leaf}\quad C_{leaf} = 0.86C_{leaf,green} + 0.24C_{leaf,brown}\,\}\quad for\ f_{LS} > 1 \qquad [42]$$

### 1.4.2 Leaf area Index ($LAI$) and stem height ($h$)

At the end of each day, the C content of the stem and leaf is used to estimate $LAI$ by eqs. [43] and [44].

$$LAI = (C_{leaf}\,/f_c) \times SLA \qquad [43]$$

where $SLA = \Upsilon\,(DVI + 0.06)^{\delta}$ [44]

The values $\Upsilon$ and $\delta$ were determined by fitting the values to the paired values of DVI and specific leaf area ($SLA$). The value of $f_c$ is 0.5 (unitless), denotes carbon fraction of dry matter.

The amount of C in the stem is used to calculate the crop height $h$ in m by eq. [45].

$$h = k\,(C_{stem}\,/f_c\,)^{\lambda} \qquad [45]$$

where $k$ and $\lambda$ were determined by fitting the value $C_{stem}$ and $h$.

### 1.4.3 Yield variables

According to (Osborne *et al.*, 2015) yield can be calculated from the C allocated to the harvest pool ($C_{harv}$) at the end of the growing season as described in eq. [46]

$$Yield_{grain} = \frac{(C_{harv}\times(1/f_c)\times D_w\times E_g)}{1000} \qquad [46]$$

Where harvested C is converted to total biomass (using the conversion factor $f_c$=0.5), i.e., by multiplying the harvested C by 1/$f_c$, and then by 1/0.84 ($D_w$) to account for the grain moisture content (Mulvaney and Devkota, 2020). $C_{harv}$ includes both chaff and grain however, $O_3$ fumigation

https://doi.org/10.5194/egusphere-2024-694
Preprint. Discussion started: 16 April 2024


experimentalists tend to only include grain when calculating total crop yield at the end of the growing season, so we assume 15% of the yield is chaff and include a grain to ear ratio, $E_g$, of 0.85. Dividing by 1000 converts yield from kg C m$^{-2}$ to g C m$^{-2}$, the unit most often used to describe experimental yield results.

Evaluation of the DO$_3$SE-crop model uses a variety of growth 'dry matter ($DM$)' metrics. Some of the most important metrics and their calculations are: '$Straw\ DM$' which is calculated as the sum of carbon allocated to $C_{stem}$, $C_{leaf}$, and $C_{resv}$; '$Ear\ DM$' is calculated from $C_{harv}$ excluding the moisture content ($D_w$) conversion; '$Grain\ DM$' is calculated from $C_{harv}$ excluding both the moisture content ($D_w$) conversion and removing the chaff fraction conversion $E_g$; '$Above\ ground\ DM$' is the $straw\ DM$ plus the $Ear\ DM$; '$Below\ ground\ DM$' is converted from $C_{root}$; and '$Harvest\ index$' is the $Gain\ DM$ divided by the $Above\ ground\ DM$. In all cases the $f_c$ conversion factor is used to convert from e.g. g C m$^{-2}$ to g $DM$ m$^{-2}$.

## 2. DO$_3$SE-Crop model calibration

### 2.1 Xiaoji China experimental dataset

The DO$_3$SE-crop model was used to analyse the O$_3$-FACE (Free Air Concentration Enrichment) experimental data collected in Xiaoji, Jiangdu, Jiangsu Province, China. This dataset includes four modern cultivars of winter wheat (*Triticum aestivum* L.) grown under ambient and elevated [O$_3$] with the elevated treatment being, on average, 25% above the ambient [O$_3$] of 45.7 ppb for the period early March/April to end of May each year. Pants were grown in fully open-air field conditions for three consecutive growing seasons over 2007 to 2009. Table 1 describes the hourly meteorological and [O$_3$] data that are required to run the DO$_3$SE-Crop model and which are provided at the Xiaoji site.

Table 1. Hourly meteorological and [O$_3$] data measured as Xiaoji required to run the DO$_3$SE-Crop

| Variable | Unit | Description | Measurement height |
|---|---|---|---|
| $PAR_{total}$ | W/m$^2$ | Direct and diffuse PAR at the top of the canopy | - |
| $T_{air}$ | ºC | Surface air temperature in degrees Celsius | 2 m |
| $VPD$ | kPa | Leaf to air vapour pressure deficit | 2 m |
| $u_z$ | m/s | Wind speed at a reference height $z$ | 2 m |
| $\rho a$ | Pa | Surface air pressure | 2 m |
| $O3_z$ | m/s | Ozone concentration at a reference height $z$ | 2 m |

The water availability is sufficient for the wheat crop so we assume there was no soil moisture stress (Feng *et al.*, 2012). Any data gaps were filled following the AgMIP-O$_3$ gap filling protocol (see S4). For large [O$_3$] data gaps (i.e. greater than 2 weeks) which occur outside the [O$_3$] fumigation period we use scaled WFRChem (version 4.2) data for Xiaoji (Conibear et al., 2018a) to ensure consistency in model calibration and potential applications across China. The four cultivars were Yannong 19 (strong-gluten wheat, hereafter Y19), Yangmai 16 (medium-gluten wheat, hereafter Y16), Yangmai 15 (weak-gluten wheat, hereafter Y15) and Yangfumai 2 (weak-gluten wheat, hereafter Y2). The dataset provides measurements of key physiological variables for the Y2 and Y16 cultivars (i.e. $A_{net}$, $V_{cmax}$, $J_{max}$ and $g_{O3}$) for the flag leaf which were used to evaluate the DO$_3$SE-Crop model's simulations of these variables.

Additional data also provide measurements of chlorophyll content Index (CCI), which can be used to assess the level of senescence experienced by the leaf (Mariën *et al.*, 2019).The dataset also

https://doi.org/10.5194/egusphere-2024-694
Preprint. Discussion started: 16 April 2024


provides grain yield components, including the number of ears per square meter, the number of grains per ear and the grain dry matter ($Grain\ DM$) (the latter in g m$^{-2}$) (Feng *et al.*, 2011, 2016). Further experimental details are provided in (Feng *et al.*, 2011, 2016).

### 2.2 DO$_3$SE-Crop calibration and evaluation

The Xiaoji experimental data were split into calibration (year 2008, Y2 and Y16 cultivars) and evaluation (year 2007 & 2009, Y15 & Y19 cultivars). The calibration of DO$_3$SE-Crop has two main steps, firstly, to calibrate for crop development and growth (i.e. phenology and C allocation). This calibration was performed using the Y2 cultivar. Secondly, the calibration of the O$_3$ damage module, this was calibrated for using the Y2 cultivar (representing a sensitive cultivar and Y16 (representing a tolerant cultivar), these cultivar sensitivities followed information provided in (Feng *et al.*, 2016).

#### Calibration

Calibration of the DO$_3$SE-Crop model used a combination of automated (for phenology) and manual (for leaf physiology, canopy C allocation and O$_3$ damage) calibration methods. Both methods require defining an initial parameter value and a realistic range over which the parameter value may vary. These parameter values are defined from a combination of observations from the Xiaoji experimental dataset as well as values taken from the literature (see supplementary Table 2 for details). The model is calibrated until certain conditions were satisfied, as explained below.

Calibration of the phenology module used the Xiaoji 2008 dataset for the Y2 cultivar. These data were used to determine the thermal life span of the canopy from sowing to maturity ($TT_{leaf}$) and calibrate key phenology parameters ($T_b$, $T_0$, $T_m$, $VT_{min}$, $VT_{max}$, $PIV$, and $PID$, flag leaf emergence, $A_{start}$ , $tl_{ep}$ and $tl_{se}$). The phenology calibration was automated by computationally applying a genetic algorithm (Wang, 1997), an optimisation technique with gradient decent to find the best parameters. This uses a combination of crossover strategy (selecting parameters randomly from parameter pairings) and mutation strategy (which takes a parameter range and uses incremental step changes) to identify the parameters which give the highest R$^2$ and lowest RMSE when compared with observations of the timing (day of year) of emergence, anthesis and maturity. The calibrated phenology parameters were tested for the other years (i.e. 2007 and 2009, including all the cultivars) to assess their ability to represent crop development between years.

We applied a sensitivity analysis to identify the leaf physiology, C allocation and O$_3$ damage module parameters that were most important to calibrate (Iwanaga et al., 2022). The sensitivity analysis identified the following DO$_3$SE-crop parameters for calibration: i). leaf photosynthesis parameters ( $V_{cmax}$, $J_{max}$, $kN$, $m$ and $VPDo$; ii). C allocation parameters ($a_{root}$, $a_{leaf}$, $a_{stem}$, $\lambda$,θ); iii). dark respiration coefficients ($R_{dcoeff}$ and $R_{gcoeff}$), and iv). O$_3$ damage module parameters related to senescence ($\gamma 3$, $\gamma 4$ and $\gamma 5$). Calibration for these parameters was performed manually and in steps; firstly, the best parameters are found for leaf photosynthesis i.e. parameters which give a maximum $A_{net}$ value of 30 µmol CO$_2$ m$^{-2}$ s$^{-1}$ and $g_{O3}$ value of 350 mmol O$_3$ m$^{-2}$ s$^{-1}$ (consistent with maximum values observed in the Xiaoji dataset, Xhu et al., 2011) . Secondly, calibration is then performed for the C allocation parameters, identifying the best parameters which meet each of the following criteria:- a stem dry matter: leaf dry matter ratio of approx. 2:1 (after (Huang *et al.*, 2022)); relative growth of different plant parts which are consistent with growth profiles found in the literature ((Osborne *et al.*, 2015)and de Vries et al., 1989); an R$^2$ value of above 0.90 when modelled $Grain\ DM$ is plotted against observed $Grain\ DM$ ; $Above\ ground\ DM$ values are between 1200-1600 g m$^{-2}$; a LAI of between 4-7 m$^2$ m$^{-2}$ and $R_d$ is 30 to 60% of the assimilated $A_{net}$(Amthor *et al.*, 2019). Finally, the model is then calibrated for the O$_3$ parameters, while other parameters remain fixed, the best calibrated parameters are those that give an R$^2$ value of above 0.90 when modelled

https://doi.org/10.5194/egusphere-2024-694
Preprint. Discussion started: 16 April 2024


$Yield_{grain}$ difference was compared against observed $Yield_{grain}$ difference for ambient versus elevated $O_3$ treatments.

Full details and description of the DO3SE-crop parameters for wheat and their associated ranges are given in Table S3, S4 and S5.

https://doi.org/10.5194/egusphere-2024-694
Preprint. Discussion started: 16 April 2024


**Results**

We first examine the model's ability to simulate the key phenological development stages since this is key to simulating the variation in C allocation over the course of the growing season and hence how $O_3$ exposure will influence growth and yield which is determined by the timing and length of the grain filling period. We also explore how $DO_3SE$-Crop simulates within canopy [$O_3$] profiles to understand which layers of the canopy are most important in determining $O_3$ response. We then examine the ability of the model to simulate leaf-level physiology and C allocation to the different parts of the crop. Lastly, the impact of both instantaneous and long-term $O_3$ damage on the crop's final grain yield is evaluated.

i) Crop Phenology

The Xiaoji dataset provides sowing and harvest dates for all cultivars for each year, however the date of the timing of anthesis is only provided for the year 2008 for all the cultivars. We assume that DVI = 1 is equivalent to the start of anthesis (and happens 4-5 days after the emergence of the flag leaf) as shown in Fig. 2. The model is calibrated using the 2008 Y2 data to provide the thermal times for $TT_{veg}$ and $TT_{rep}$ and uses the CCI data and associated breakpoint method to estimate $tl_{ep}$ and $tl_{se}$. We then assume that these values are consistent across cultivars and years. Figure S1 shows the timing of crop emergence, anthesis and harvest in relation to simulated anthesis (i.e. at DVI=1). There is a variation of 4 to 10 days for anthesis in relation to days from crop emergence between years. The $T_l$ ranges between 1325 and 1478 °C days for the three years with crop emergence occurring between day of year 37-45 and harvest occurring between day of year 135-151. The number of days from crop emergence to harvest was between 100 and 104 for the three years.

ii) Within canopy stomatal $O_3$ profile

An important determinant of $O_3$ deposition and damage is stomatal $O_3$ deposition (or stomatal $O_3$ uptake) which is a function of within canopy transfer of $O_3$ and stomatal and non-stomatal deposition. The multi-layer aspect of the $DO_3SE$-Crop model allows within canopy stomatal and non-stomatal $O_3$ deposition to be simulated. Figure 3 shows the variation in key variables that determine total and stomatal $O_3$ canopy deposition across 4 canopy layers as a mid-day average over the course of the $tl_{ep}$ period of the flag leaf, for the year 2008 and the Y2 cultivar.

Figure 3. Plot showing variation in key $O_3$ deposition terms as daily maxima by canopy layer (N.B. $i = 1$ is the top canopy layer, $n = 4$) a). [$O_3$], b). $rb_{,O3}$, c). $PAR_{sun}$ and d). $g_{O3}$ for the duration of the flag leaf period for the Y2 cultivar E-$O_3$ treatment in 2008.

a). b).

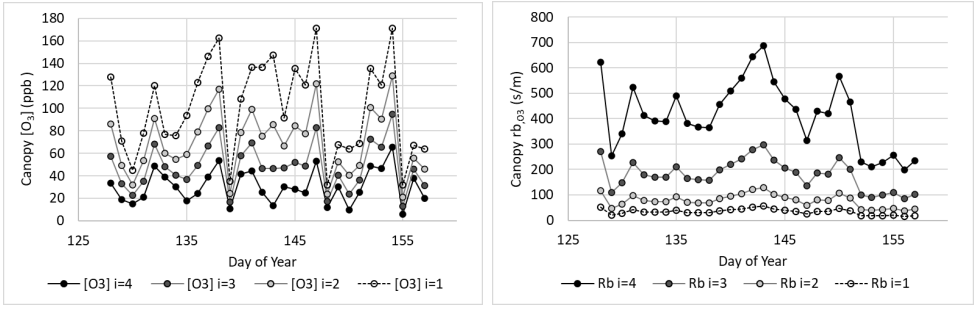

https://doi.org/10.5194/egusphere-2024-694
Preprint. Discussion started: 16 April 2024


c). d).

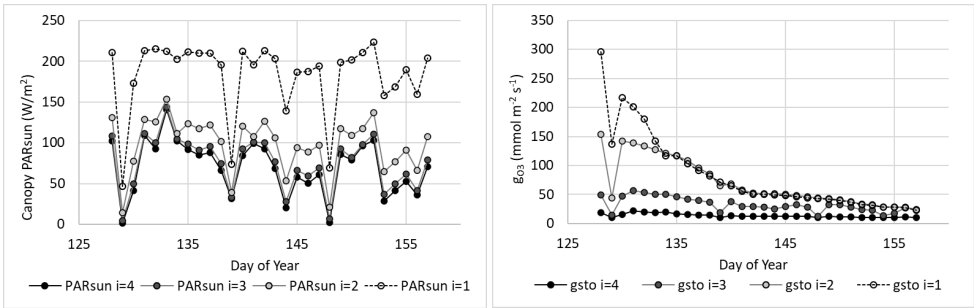


Figure 3a. shows a decrease of within canopy [$O_3$] from highs of around 140ppb to values within the range of 10 to 50 ppb between the topmost and bottom canopy layer. Similarly, $PAR_{sun}$ reduces from maximum values of around 200 W m$^{-2}$ to values of around 100 W m$^{-2}$ on sunny days (see Fig. 3b). The leaf $rb_{O3}$ (Fig. 3c) also increases with canopy depth from resistances in the region of approximately 100 s m$^{-1}$; and $g_{O3}$ (Fig. 3d) similarly reduces from around 300 to 20 nmol $O_3$ m$^{-2}$ s$^{-1}$ between canopy layers, these differences reduce with the onset of senescence.

iii) Leaf physiology variables ($A_{net}$, $g_{sto}$)

The $DO_3SE$-Crop model was able to simulate the seasonal $A_{net}$ and $g_{O3}$ with values ranging from 0 and 27 and 10 and 310 for $A_{net}$and $g_{O3}$ respectively over the course of the growing season (see Fig. 4). The simulated daily maximum values of modelled $g_{O3}$, of 310 mmolm$^{-2}$ s$^{-1}$ were in the range of the observed value of 340 mmol $O_3$ m$^{-2}$ s$^{-1}$. Similarly, the modelled maximum $A_{net}$ is 27 µmol $CO_2$ m$^{-2}$ s$^{-1}$ compared to observed value of 28 µmol $CO_2$ m$^{-2}$ s$^{-1}$ for the period between anthesis and 10 days before maturity for the year 2008, for both the Y2 and Y16 cultivar.

Fig 4. $DO_3SE$-Crop modelled diurnal profile of a). $g_{O3}$, and b). $A_{net}$ for a fully-expanded flag leaf prior to the start of senescence $tl_{ep}$ for the AA and seasonal profile of daily maxima c). $g_{O3}$, and d). $A_{net}$ for the flag leaf between $tl_{ep}$ and $tl_{se}$ for the AA treatments. Black line showing the Start of senescence (SOS)

a). b).

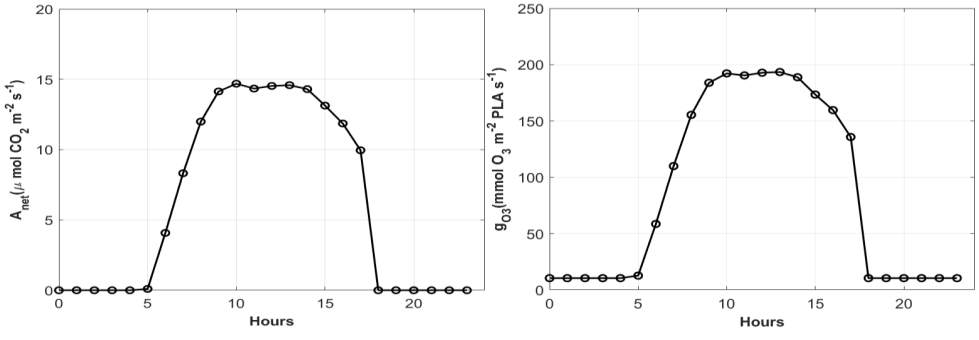

https://doi.org/10.5194/egusphere-2024-694
Preprint. Discussion started: 16 April 2024


c). d).

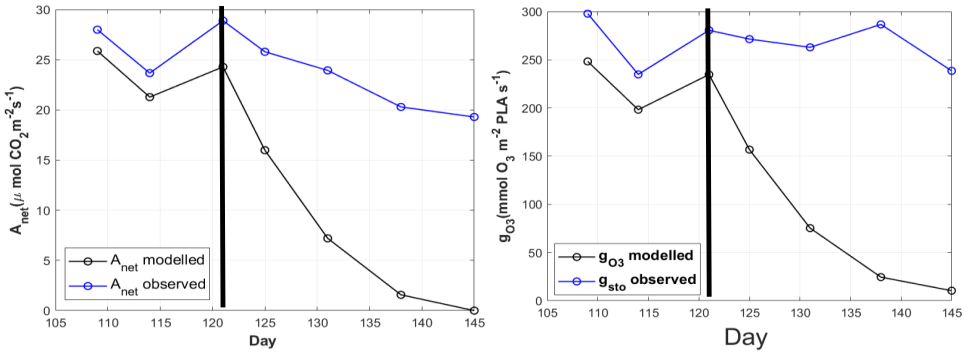


iv) Crop growth and yield.

The dry matter dynamics of the different parts of the crop are shown in Fig. 5. The modelled $Grain\ DM$ value of 843 g $m^{-2}$ matched the observed value of 876 g $m^{-2}$. The stem-to-leaf ratio is 2.1:1, in the range provided in the literature (Huang *et al.*, 2022). Above-ground biomass values of 1510 g $m^{-2}$ also match well against the 1200-1600 g $m^{-2}$ range described in the literature (Huang *et al.*, 2022; Liu *et al.*, 2022). Further, the partition fraction profiles are consistent with those of (Osborne *et al.*, 2015)(see Fig. 5); the main differences are that the modelled stem and root partition profiles are somewhat higher and lower, respectively, as compared to (Osborne *et al.*, 2015).

Figure 5 a). the partition fractions of the daily accumulated $NPP$ partitioned to roots, stems, leaves, and grains for modelled (solid lines) *vs* the JULES Crop model (dashed line after (Osborne *et al.*, 2015)) plotted against $DVI$, and b). the $DM$ of daily accumulated $NPP$ partitioned to roots, stems, leaves, and grains plotted against $DVI$.

a). b

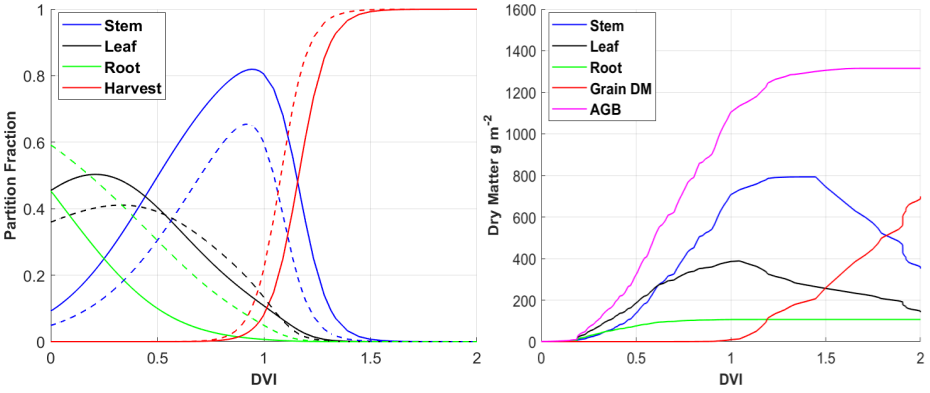


v) Instantaneous and long-term $O_3$ impact

The $Yield_{grain}$ is assumed to be damaged by both the instantaneous impact of $O_3$ (Farage *et al.*, 1991) on photosynthesis as well as the long-term $O_3$ effect that can lead to enhanced senescence (Feng *et al.*, 2022).To explore which of these damage mechanisms is most important we calculated the difference between the C accumulation that would be partitioned to the grain for the AA and E-$O_3$ treatment as compared to a simulated very low [$O_3$] treatment representing pre-industrial

https://doi.org/10.5194/egusphere-2024-694
Preprint. Discussion started: 16 April 2024


conditions for both the tolerant (Y16) and sensitive (Y2) cultivar for each of the three years (see Table 1). We found a negligible effect of $O_3$ (0-0.2 %) on C allocations due to the instantaneous effect of $O_3$ on photosynthesis compared to a highly significant (2.86-35.85 %) impact due to the long-term $O_3$ effect *via* the enhancement of senescence on final $Yield_{grain}$.

Table 1. The modelled % $Yield_{grain}$ loss compared to a pre-industrial $O_3$ scenario divided between that $Yield_{grain}$ loss caused by the direct and instantaneous effect of [$O_3$] on photosynthesis and that due to the long-term [$O_3$] impact on senescence.

| **Year** | **Tolerant: Instantaneous $O_3$ effect on % $Yield_{grain}$** | | **Tolerant: Long-term $O_3$ effect on % $Yield_{grain}$** | |
|---|---|---|---|---|
| | Ambient versus pre-industrial | Elevated versus pre-industrial | Ambient versus pre-industrial | Elevated versus pre-industrial |
| 2007 | 0.01 | 0.01 | 2.86 | 6.6 |
| 2008 | 0 | 0 | 3.29 | 17.57 |
| 2009 | 0.03 | 0.03 | 6.40 | 25.41 |
| | **Sensitive: Instantaneous $O_3$ effect on % $Yield_{grain}$** | | **Sensitive: Long-term $O_3$ effect on % $Yield_{grain}$** | |
| | Ambient versus pre-industrial | Elevated versus pre-industrial | Ambient versus pre-industrial | Elevated versus pre-industrial |
| 2007 | 0 | 0.2 | 5.84 | 12.48 |
| 2008 | 0 | 0 | 5.21 | 26.5 |
| 2009 | 0.01 | 0.01 | 13.50 | 35.85 |

vi) Senescence

The breakpoint method (Mariën *et al.*, 2019) was used to determine the onset (SOS) and end (EOS) of senescence and maturity respectively using the chlorophyll content index (CCI) data which was available for the year 2008, and the Y2 and Y16 cultivars. Results showed (Fig. 6) that the E-$O_3$ treatment for cultivars Y2 and Y16 brought forwards the SOS by 9 and 7 days respectively, and EOS by 4 and 2 days respectively.

Figure 6. Leaf senescence profiles of $O_3$ induced leaf senescence for the Y2 cultivar for the a).ambient (AA) and b).elevated (E-$O_3$) $O_3$. The timing of the SOS (solid black line) and EOS (dashed black line) were determined by applying the break point method to the CCI data and are shown in relation to the $f_{LS}$ simulations of senescence (grey line). The observed relative CCI data are also shown (open symbols)

https://doi.org/10.5194/egusphere-2024-694
Preprint. Discussion started: 16 April 2024


a). b).

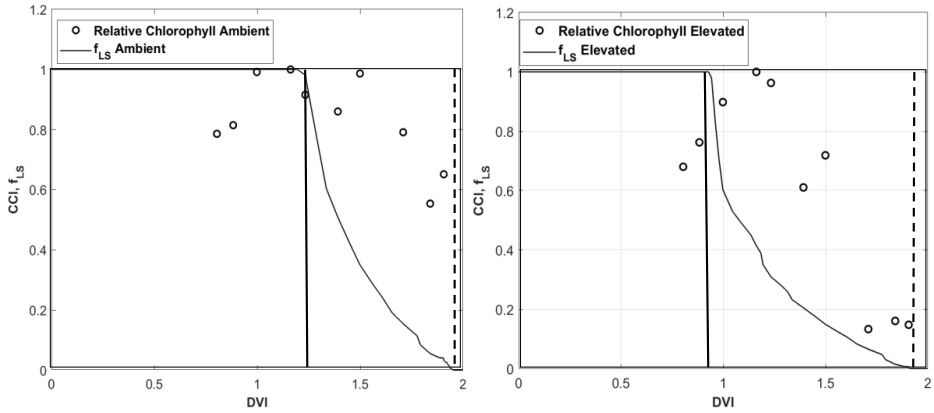


vii) Simulations across years and between cultivars

Figure 7 shows a box plot of the modelled *vs* observed $Yield_{grain}$ for both the sensitive (Y2) and tolerant (Y16) cultivars for each $O_3$ treatment (AA and E-O3), for the years 2007, 2008 and 2009. The model simulates the difference in $Yield_{grain}$ between the AA and E-$O_3$ reasonably well with a simulated reduction in $Yield_{grain}$ of 29 and 131 g m$^{-2}$ compared with observed 81 and 165 g m$^{-2}$ for the tolerant and as 49 and 196 g m$^{-2}$ compared with observed 54 and 293 g m$^{-2}$sensitive cultivars respectively. The most notable difference is that there is a larger range in the simulated $Yield_{grain}$ losses of the modelled sensitive cultivar though the mean value is more conservative at 610 g m$^{-2}$ *vs* an observed value of 590 g m$^{-2}$.

Fig 7. Boxplots (crosses: 0.01 and 0.99 percentiles; box: 0.25 quartile, median and 0.75 quartile; square: mean) of simulated and observed wheat $Yield_{grain}$ for the tolerant (Y15 and Y16) and sensitive (Y2 and Y19) cultivars under AA and E-$O_3$ conditions in the years 2007, 2008 and 2009.

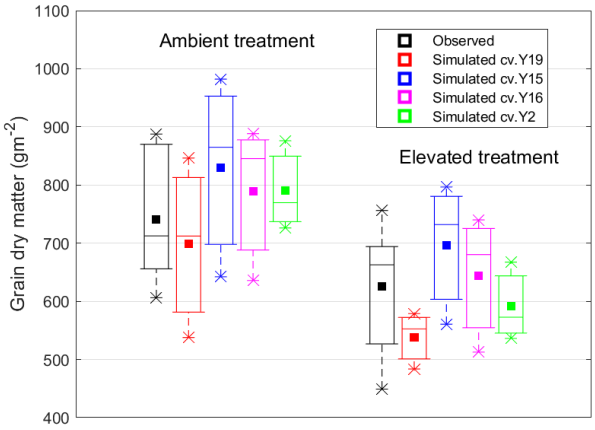


Figure 8 shows the relationship between modelled *vs* observed $Yield_{grain}$ (in g m$^{-2}$), a linear regression through these data gives an $R^2$ value of 0.73, showing the model is able to simulate the differences in absolute yield for different cultivars and for different years reasonably well. The data

https://doi.org/10.5194/egusphere-2024-694
Preprint. Discussion started: 16 April 2024


points for 2007 overestimated the $Yield_{grain}$ for the E-$O_3$ treatments i.e. underestimating the yield loss, this was due to the $O_3$ treatment period being substantially shorter for the year 2007 compared to the other years (i.e. 2008 and 2009) by 38 days compared to 92 days.

Fig. 8 A scatter plot showing modelled vs observed $Yield_{grain}$ (in g $m^{-2}$) for all 4 cultivars and 3 years of the Xiaoji dataset.

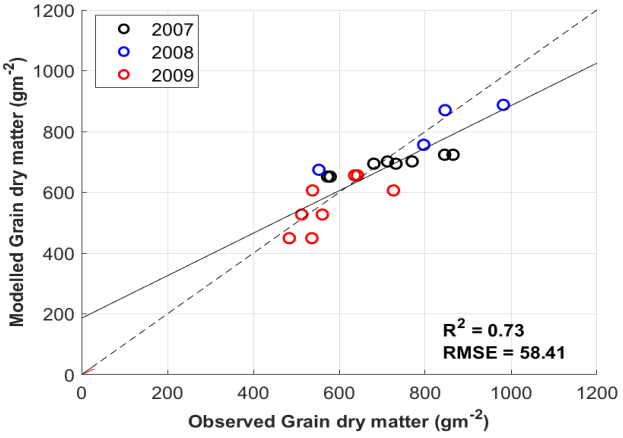

https://doi.org/10.5194/egusphere-2024-694
Preprint. Discussion started: 16 April 2024


**Discussion**

The $DO_3SE$-Crop model was found capable of simulating $O_3$ damage to grain yield for $O_3$-FACE conditions at the experimental site in Xiaoji, China. Simulated yield losses between ambient and elevated $O_3$ conditions for all years ranged between 4-19% and 7-25% for tolerant and sensitive cultivars respectively, these simulated values are close to equivalent observed value ranges of between 12-19% and 10-34%. However, it should be noted that the model overestimated grain dry matter for the elevated $O_3$ treatments for the year 2007 (see Fig. 5) due to a shorter exposure period. (Zhu *et al.*, 2011) argued that despite the delayed and shorter $O_3$ fumigation period in 2007, the elevated $O_3$ levels were not much less than in other seasons and concluded this was the reason for the same level of $O_3$ impact on experimental grain yield. However, the accumulated stomatal $O_3$ flux estimated by the $DO_3SE$-model was much higher for the elevated $O_3$ treatment for the years 2008 and 2009 (at ~ 19 mmol $O_3$ $m^{-2}$) compared to 2007 (16.3 mmol $O_3$ $m^{-2}$), hence the greater modelled impact on the relative grain yield loss (15-18% for 2008 and 2009 versus 4-6% for 2007).

Overall, the $DO_3SE$ model simulation results compare favourably to results made by the MCWLA-Wheat model (Tao *et al.*, 2017) which was also calibrated for the Xiaoji experimental conditions but without distinction between tolerant and sensitive varieties; MCWLA-Wheat absolute simulated yield varied between ~5700 and 9000 kg/ha (compared to ~5700 to 9800 kg/ha) for ambient and ~4800 to 8000 kg/ha (compared to ~5200 to 8000) for elevated $O_3$ treatments. A mean relative yield loss of 14% was simulated by the model. For context, mean relative yield losses across East Asia were estimated at 33% (with a mean range of 28-37%) by (Feng *et al.*, 2022) according to a mean monitored [$O_3$] of 30.9 ppm h expressed as AOT40 (six-month accumulated daytime O3 concentration above a threshold of 40 ppb). The mean difference in AOT40 (accumulated over only 75 days) between the ambient and E-O3 treatments at Xiaoji across all years was 7.8 ppm h.

Crop phenology plays a crucial role in determining the entire $O_3$ exposure period (i.e., from crop emergence to maturity), and hence $O_3$ damage since steady $O_3$ accumulation ($acc_{fst}$) occurring from early on in the crop growth period can cause $O_3$ detoxification mechanisms to be overwhelmed. The $DO_3SE$-crop model simulates the crop phenology for the three years at Xiaoji well compared to the observed dataset ($R^2$ =0.98, see Fig. S1). Estimating the correct timing of anthesis is crucial since the period from anthesis to crop maturity is the $O_3$-sensitive period. During this period, accumulated stomatal $O_3$ flux ($acc_{fst}$) will contribute to early and enhanced senescence once the critical threshold ($CLsO3$) is exceeded. This period also coincides with C accumulation in the grain (Kohut, Amundson and Laurence, 1987; Feng, Kobayashi and Ainsworth, 2008) which may be limited by $O_3$-induced early onset or enhanced senescence. The $DO_3SE$-crop model was developed to accommodate the full range of effects of $O_3$ on senescence with revised (Ewert and Porter, 2000)functions able to modify both the $O_3$ induced onset of senescence as well as the $O_3$ effect on maturity. This is important since experimental evidence has shown that $O_3$ can bring forward the maturity date; for example, the flag leaf was found to have senesced 25 days earlier in a high [O3], compared to a charcoal-filtered treatment (Grandjean and Fuhrer Grandjean, 1989; Gelang *et al.*, 2000). $O_3$ was also found to cause differences in the time to maturity of the flag leaf, with Shi et al. (2009) reporting that maturity was brought forward by eight days in an elevated $O_3$ (50% higher than ambient) treatment. Currently, other crop models with $O_3$ damage functions (e.g. MLCWLA-Wheat (Tao *et al.*, 2017)and LINTULLCC-22 (Feng *et al.*, 2022)are only able to bring the $O_3$-induced onset of senescence earlier.

The $DO_3SE$-crop model is also able to simulate differential $O_3$ uptake in each canopy layer. Fig. 3 shows that the majority of stomatal $O_3$ uptake occurs in the sunlit layers of the upper canopy. Similar results were found in an experimental study on a productive grassland in Switzerland (Jaggi *et al.*,

https://doi.org/10.5194/egusphere-2024-694
Preprint. Discussion started: 16 April 2024


2006) who found that different levels of $O_3$ exposure to canopy components predominantly located in the upper and lower parts of the canopy support a multi-layer approach to modelling $O_3$ uptake. Therefore, the focus on the upper canopy by flux-based $O_3$ metrics (e.g. the phytotoxic ozone dose $POD_y$ (UNECE, 2017) seems rational in the absence of multi-layer modelling. Crop models such as LINTULCC-2 (Feng *et al.*, 2022)also focus on estimating stomatal $O_3$ uptake at the top of the canopy to estimate $O_3$ induced yield losses. For wheat, such an approach is further supported by the facts that the upper canopy layers consist of the flag leaf, which plays a crucial role in photosynthesis and grain filling (Pleijel *et al.*, 2007).

Our results show that the $DO_3SE$-crop model was able to estimate the seasonal course of $A_{net}$ and $g_{O3}$ daily maxima observed at the Xiaoji site (see Fig. 4a) as well as being able to produce reasonable diurnal profiles for $A_{net}$ and $g_{O3}$ (see Fig. 4b) when compared to other literature describing leaf physiological variables (Guan *et al.*, 2015; Li *et al.*, 2022). This suggests the coupled $A_{net}g_{sto}$ model is working for Chinese conditions (having previously been applied and evaluated for European $O_3$ experimental conditions – see Pande et al. sub). The leaf physiology parameters used in this study (i.e. for Asian conditions and cultivars) are higher than parameters for European studies. For Europe, $V_{cmax}$ values of between 60 and 90 µmol $CO_2$ $m^{-2}$ $s^{-1}$ were found in the literature (Feng et al., 2022; Pande et.al., sub, Van Oijen and Ewert, 1999) compared to the observed mean maximum value of 137 µmol $CO_2$ $m^{-2}$ $s^{-1}$ at Xiaoji which was used in this study. Similarly, European $J_{max}$ values ranged from 160 to 180 µmol $CO_2$ $m^{-2}$ $s^{-1}$ (Feng et al., 2021, Pande et al. sub, Van Oijen & Ewert, 1999) compared to the observed Xiaoji mean maximum value of 228 µmol $CO_2$ $m^{-2}$ $s^{-1}$.

Ensuring the seasonal variation in C allocation to the different components of the crop (i.e. roots, stem, leaves and harvest organs) is essential for the simulation of crop growth and yield. There are few data in the literature that provide these variables so we compare our results to the C allocation profiles described for wheat provided in the original JULES Crop model description, recognising this is intended for wheat grown globally. The $DO_3SE$-Crop model C allocation to the stem and roots is comparatively higher than was simulated by JULES Crop ((Osborne *et al.*, 2015); see Fig. 5a). However, we can justify the C allocation coefficients we used for Xiaoji since the $DO_3SE$-Crop model was able to distribute C to different plant components to produce a well-proportioned plant over the course of the growing season, this was determined by the calibration to a number of key crop variables (i.e. ratios of plant respiration, $LAI$, stem to leaf dry matter ratios, above ground components and grain dry matter. Importantly, the model, was found to simulate the grain dry matter for the year 2008 and the cultivar Y16 (tolerant) & Y2(sensitive) under the ambient and elevated $O_3$ treatment to within 0.08- 2.19% of the observed values ($R^2$ =0.99, 9.27 g/m² see Fig. S2).

The $DO_3SE$-Crop model, similar to other crop models with $O_3$ damage functions (i.e. MLCWLA-Wheat (Tao *et al.*, 2017)and LINTULLCC-2 (Feng *et al.*, 2022)) has the capacity to simulate both the instantaneous and long-term $O_3$ impact on wheat grain yield. The instantaneous $O_3$ effect on photosynthesis may cause leaf cell damage and decrease the supply of carbohydrate precursors which can significantly decrease $g_{O3}$, $V_{cmax}$ and leaf chlorophyll content (Farage *et al.*, 1991). Elevated $O_3$ also leads to generation of reactive oxygen species (ROS) in plant cells which can cause oxidative damage to various cellular components. Rubisco, the enzyme responsible for C fixation in the photosynthetic process, can be particularly susceptible to this damage, leading to a reduced carboxylation rate ($V_{cmax}$). Such an ozone effect on $V_{cmax}$ reduces net photosynthesis and can also induce early senescence shortening the grain filling period (Triboi and Triboi-Blondel, 2002). Results from the $DO_3SE$-crop model found a larger impact on yield due to the long-term $O_3$ impact causing relative yield loss of between 2 to 36% compared to only 0 to 0.2% resulting from the instantaneous $O_3$ impact on photosynthesis. Previous studies have also found that the long-term $O_3$ effect has a larger impact on yield compared to the instantaneous effect of $O_3$ on photosynthesis (Emberson *et al.*, 2018; Brewster, Fenner and Hayes, 2024). Senescence is an age-dependent process

https://doi.org/10.5194/egusphere-2024-694
Preprint. Discussion started: 16 April 2024


of degradation and degeneration that allows nutrients to be re-distributed to different plant organs (Lim et al., 2007). Under $O_3$ stress, this process is often found to occur earlier and more rapidly in leaves as well as at the whole plant or crop canopy scale (Brewster, Fenner and Hayes, 2024). The causes of this early and accelerated senescence are not completely understood but may be related to $O_3$ induced enhanced expression of many genes involved in natural senescence (Miller, Arteca and Pell, 1999). Elevated $O_3$ was also found to inhibit sugar export from leaves (Singh Yadav *et al.*, 2020; Feng *et al.*, 2024) which could trigger early onset of leaf senescence.

The $DO_3SE$-crop model accounts for the impact of $O_3$ on the Rubisco enzyme by incorporating modified (Ewert and Porter, 2000) functions for instantaneous and long-term $O_3$ impact on $V_{cmax}$ as an important parameter used to characterize the crop photosynthetic capacity (Ewert and Porter, 2000; Osborne *et al.*, 2019). The $DO_3SE$-crop model assumes that the $O_3$ will only accumulate on exceedance of a stomatal $O_3$ flux threshold of 6 nmol $O_3$ $m^{-2}$ $s^{-1}$. The long-term $O_3$ impact mechanism of the DO3SE-crop model simulated the effect of senescence on $V_{cmax}$ reasonably well as evidenced by the reduction in leaf chlorophyll content. We used the breakpoint method (Yang *et al.*, no date; Mariën *et al.*, 2019)to estimate the SOS and EOS using measured chlorophyll content index values and. It is crucial to accurately model the timing of SOS and EOS correctly as this determines the $O_3$ effect on the duration of the grain filling period and hence the difference in yield loss due to different $O_3$ treatments. For example, we modelled a difference of 8 and 3 and 4 and 1 days in SOS &EOS respectively on average across years for the sensitive and tolerant cultivar respectively.

China's wheat breeding programme has seen more than 1,850 varieties used across China between the 1920s to 2014 leading to increased yields from less than <1 to >5 tonnes $ha^{-1}$ (Qin *et al.*, 2015). Here, albeit with an extremely limited dataset, we parameterise the $DO_3SE$-crop model for tolerant and sensitive wheat crop cultivars, since many experimental studies have shown that the response of different cultivars to $O_3$ stress differs (Biswas *et al.*, 2008). Based on the available data the model seemed able to capture the difference in grain dry matter between these different cultivar groups across different years reasonably well when compared against the observed dataset ($R^2$ =0.73; see Fig. 8). Such a cultivar sensitivity-based parametrisation can provide additional some information on the certainty of regional yield loss estimates given the large number of wheat varieties grown across China.

https://doi.org/10.5194/egusphere-2024-694
Preprint. Discussion started: 16 April 2024


## Conclusions

We have shown that the newly developed $DO_3SE$-Crop model can be calibrated for $O_3$ tolerant and sensitive wheat varieties for O3-FACE site conditions at Xioaji in China. The model is able to simulate crop phenology, leaf physiology, crop growth and yield well across different years. The model is also able to simulate the effect of $O_3$ stress on grain yield distinguishing the extent of $O_3$ damage resulting from the same $O_3$ treatment on cultivars with differing O3 sensitivities. The $DO_3SE$-Crop model also has the advantage of simulating $O_3$ transfer and deposition dynamics within the wheat crop canopy which could in the future improve our understanding of whole canopy $O_3$ effects. The ability of the model to estimate relative yield losses across years also suggests the model is 'fit for purpose' to assess the effects of $O_3$ under a variety of climate variable and [$O_3$] conditions.

https://doi.org/10.5194/egusphere-2024-694
Preprint. Discussion started: 16 April 2024


**References**

Amthor, J. S. *et al.* (2019) 'Engineering strategies to boost crop productivity by cutting respiratory carbon loss', *Plant Cell*, 31(2), pp. 297–314. doi: 10.1105/tpc.18.00743.

Betzelberger, A. M. *et al.* (2012) 'Ozone exposure response for U.S. soybean cultivars: Linear reductions in photosynthetic potential, biomass, and yield', *Plant Physiology*. American Society of Plant Biologists, 160(4), pp. 1827–1839. doi: 10.1104/pp.112.205591.

Biswas, D. K. *et al.* (2008) 'Assessing the genetic relatedness of higher ozone sensitivity of modern wheat to its wild and cultivated progenitors/relatives', *Journal of experimental botany*. J Exp Bot, 59(4), pp. 951–963. doi: 10.1093/JXB/ERN022.

Brewster, C., Fenner, N. and Hayes, F. (2024) 'Chronic ozone exposure affects nitrogen remobilization in wheat at key growth stages', *Science of The Total Environment*. Elsevier B.V., 908(August 2023), p. 168288. doi: 10.1016/j.scitotenv.2023.168288.

Brewster, C., Hayes, F. and Fenner, N. (2019) 'Ozone Tolerance Found in Aegilops tauschii and Primary Synthetic Hexaploid Wheat', *Plants 2019, Vol. 8, Page 195*. Multidisciplinary Digital Publishing Institute, 8(7), p. 195. doi: 10.3390/PLANTS8070195.

Campbell, G.S., Norman, J. M. (1998) *An introduction to Environmental Biophysics*. Second. Springer.

Challinor, A. J. *et al.* (2014) 'A meta-analysis of crop yield under climate change and adaptation', *Nature Climate Change*, 4(4), pp. 287–291. doi: 10.1038/nclimate2153.

Clark, D. B. *et al.* (2011) 'The Joint UK Land Environment Simulator (JULES), model description – Part 2: Carbon fluxes and vegetation dynamics', *Geoscientific Model Development*, 4(3), pp. 701–722. doi: 10.5194/gmd-4-701-2011.

Danielsson, H. *et al.* (2003) 'Ozone uptake modelling and flux-response relationships - An assessment of ozone-induced yield loss in spring wheat', *Atmospheric Environment*. Pergamon, 37(4), pp. 475–485. doi: 10.1016/S1352-2310(02)00924-X.

Emberson, L.D., Ashmore, M.R., Simpson, D., Tuovinen, J.-P. and Cambridge, H. M. (2001) 'Modelling and mapping ozone deposition in Europe', *Water, Air and Soil Pollution*, pp. 577–582.

Emberson, L. D. *et al.* (2000) 'Modelling stomatal ozone flux across Europe', *Environmental Pollution*, 109(3), pp. 403–413. doi: 10.1016/S0269-7491(00)00043-9.

Emberson, L. D. *et al.* (2018) 'Ozone effects on crops and consideration in crop models', *European Journal of Agronomy*. Elsevier, 100(May), pp. 19–34. doi: 10.1016/j.eja.2018.06.002.

Ewert, F. and Porter, J. R. (2000) 'Ozone effects on wheat in relation to CO2: Modelling short-term and long-term responses of leaf photosynthesis and leaf duration', *Global Change Biology*, 6(7), pp. 735–750. doi: 10.1046/j.1365-2486.2000.00351.x.

Farage, P. K. *et al.* (1991) 'The sequence of change within the photosynthetic apparatus of wheat following short-term exposure to ozone', *Plant Physiology*, 95(2), pp. 529–535. doi: 10.1104/pp.95.2.529.

Farquhar, G.D., von Caemmerer, S., Berry, J. A. (1980) 'A biochemical model of photosynthetic CO2 assimilation in leaves of C3 species', *Planta*, 149, pp. 78–90.

Farquhar, G. D., Caemmerer, S. and Berry, J. A. (1980) 'A biochemical model of photosynthetic $CO_2$ assimilation in leaves of $C_3$ species', *Planta*, 149(1), pp. 78-90–90. Available at: http://dx.doi.org/10.1007/BF00386231.

https://doi.org/10.5194/egusphere-2024-694
Preprint. Discussion started: 16 April 2024


Feng, Y. *et al.* (2022) 'Identifying and modelling key physiological traits that confer tolerance or sensitivity to ozone in winter wheat', *Environmental Pollution*. Elsevier Ltd, 304(April), p. 119251. doi: 10.1016/j.envpol.2022.119251.

Feng, Y. *et al.* (2024) 'Alteration of carbon and nitrogen allocation in winter wheat under elevated ozone', *Plant Science*. Elsevier, 338, p. 111924. doi: 10.1016/J.PLANTSCI.2023.111924.

Feng, Z. *et al.* (2011) 'Differential responses in two varieties of winter wheat to elevated ozone concentration under fully open-air field conditions', *Global Change Biology*, 17(1), pp. 580–591. doi: 10.1111/J.1365-2486.2010.02184.X.

Feng, Z. *et al.* (2012) 'A stomatal ozone flux-response relationship to assess ozone-induced yield loss of winter wheat in subtropical China', *Environmental Pollution*. Elsevier Ltd, 164, pp. 16–23. doi: 10.1016/j.envpol.2012.01.014.

Feng, Z. *et al.* (2016) 'Differential effects of ozone on photosynthesis of winter wheat among cultivars depend on antioxidative enzymes rather than stomatal conductance', *The Science of the total environment*. Sci Total Environ, 572, pp. 404–411. doi: 10.1016/J.SCITOTENV.2016.08.083.

Feng, Z. *et al.* (2018) 'Comparison of crop yield sensitivity to ozone between open-top chamber and free-air experiments', *Global Change Biology*. Blackwell Publishing Ltd, 24(6), pp. 2231–2238. doi: 10.1111/gcb.14077.

Feng, Z. *et al.* (2021) 'Emerging challenges of ozone impacts on asian plants: actions are needed to protect ecosystem health'. doi: 10.1080/20964129.2021.1911602.

Feng, Z., Kobayashi, K. and Ainsworth, E. A. (2008) 'Impact of elevated ozone concentration on growth, physiology, and yield of wheat (Triticum aestivum L.): A meta-analysis', *Global Change Biology*, 14(11), pp. 2696–2708. doi: 10.1111/j.1365-2486.2008.01673.x.

Gelang, J. *et al.* (2000) 'Rate and duration of grain filling in relation to flag leaf senescence and grain yield in spring wheat (Triticum aestivum) exposed to different concentrations of ozone', *Physiologia Plantarum*, 110(3), pp. 366–375. doi: 10.1111/J.1399-3054.2000.1100311.X.

Graham, A. M. *et al.* (2020) 'Impact on air quality and health due to the Saddleworth Moor fire in northern England', *Environmental Research Letters*, 15(7). doi: 10.1088/1748-9326/ab8496.

Graham, A. M. *et al.* (2021) 'Impact of the 2019/2020 Australian Megafires on Air Quality and Health', *GeoHealth*, 5(10), pp. 1–17. doi: 10.1029/2021GH000454.

Grandjean, A. and Fuhrer Grandjean, J. (1989) *Growth and leaf senescence in spring wheat (Triticum aestivum) grown at different ozone concentrations in open-top field chambers*.

Guan, X. K. *et al.* (2015) 'Effect of Drought on the Gas Exchange, Chlorophyll Fluorescence and Yield of Six Different-Era Spring Wheat Cultivars', *Journal of Agronomy and Crop Science*, 201(4), pp. 253–266. doi: 10.1111/jac.12103.

Huang, H. *et al.* (2022) 'A dataset of winter wheat aboveground biomass in China during 2007–2015 based on data assimilation', *Scientific Data*. Springer US, 9(1), pp. 1–11. doi: 10.1038/s41597-022-01305-6.

Jaggi, M. *et al.* (2006) 'Environmental control of profiles of ozone concentration in a grassland canopy', *Atmospheric Environment*, 40(28), pp. 5496–5507. doi: 10.1016/j.atmosenv.2006.01.025.

Jones, H. G. (1992) *Plants and microclimate: A quamntitative approach to environmental plant physiology*. Cambridge University Press.

Kohut, R. J., Amundson, R. G. and Laurence, J. A. (1987) 'Effects of ozone and sulfur dioxide on yield

https://doi.org/10.5194/egusphere-2024-694
Preprint. Discussion started: 16 April 2024


of winter wheat', *Phytopathology*, 77(1), pp. 71–74. doi: 10.1094/Phyto-77-71.

Konduri, V. S. *et al.* (2020) 'Data Science for Weather Impacts on Crop Yield', *Frontiers in Sustainable Food Systems*, 4(May). doi: 10.3389/fsufs.2020.00052.

Lee, J. D. *et al.* (2020) 'UK surface NO2 levels dropped by 42 % during the COVID-19 lockdown: Impact on surface O3', *Atmospheric Chemistry and Physics*, 20(24), pp. 15743–15759. doi: 10.5194/acp-20-15743-2020.

Leung, F. *et al.* (2020) 'Calibrating soybean parameters in JULES 5.0 from the US-Ne2/3 FLUXNET sites and the SoyFACE-O3 experiment', *Geoscientific Model Development*. Copernicus GmbH, 13(12), pp. 6201–6213. doi: 10.5194/GMD-13-6201-2020.

Leuning, R. (1990) 'MODELING STOMATAL BEHAVIOR AND PHOTOSYNTHESIS OF EUCALYPTUS-GRANDIS', *AUSTRALIAN JOURNAL OF PLANT PHYSIOLOGY*, 17(2), pp. 159–175.

Leuning, R. (1995) 'A critical appraisal of combine stomatal model C3 plants', *Plant, Cell & Environment*, 18, pp. 339–355. Available at: http://www.unc.edu/courses/2010spring/geog/595/001/www/Leuning95b-PCE.pdf%0Apapers2://publication/uuid/B8B998AB-EB42-4E09-A609-B192084D13EE.

Li, A., Zhou, Q. and Xu, Q. (2021) 'Prospects for ozone pollution control in China: An epidemiological perspective', *Environmental Pollution*. Elsevier Ltd, 285. doi: 10.1016/J.ENVPOL.2021.117670.

Li, D. *et al.* (2022) 'Surface ozone impacts on major crop production in China from 2010 to 2017', *Atmospheric Chemistry and Physics*, 22(4), pp. 2625–2638. doi: 10.5194/acp-22-2625-2022.

Li, K. *et al.* (2020) 'anthropogenic and meteorological influences', *Atmos. Chem. Phys*, 20, pp. 11423–11433. doi: 10.5194/acp-20-11423-2020.

Lin, M. *et al.* (2017) 'US surface ozone trends and extremes from 1980 to 2014: Quantifying the roles of rising Asian emissions, domestic controls, wildfires, and climate', *Atmospheric Chemistry and Physics*, 17(4), pp. 2943–2970. doi: 10.5194/acp-17-2943-2017.

Liu, S. *et al.* (2010) 'Crop yield responses to climate change in the Huang-Huai-Hai Plain of China', *Agricultural Water Management*. Elsevier, 97(8), pp. 1195–1209. doi: 10.1016/J.AGWAT.2010.03.001.

Liu, Z. *et al.* (2022) 'Tropospheric ozone changes and ozone sensitivity from the present day to the future under shared socio-economic pathways', *Atmospheric Chemistry and Physics*. Copernicus GmbH, 22(2), pp. 1209–1227. doi: 10.5194/ACP-22-1209-2022.

Malhi, G. S., Kaur, M. and Kaushik, P. (2021) 'Impact of Climate Change on Agriculture and Its Mitigation Strategies: A Review', *Sustainability 2021, Vol. 13, Page 1318*. Multidisciplinary Digital Publishing Institute, 13(3), p. 1318. doi: 10.3390/SU13031318.

Mariën, B. *et al.* (2019) 'Detecting the onset of autumn leaf senescence in deciduous forest trees of the temperate zone', *New Phytologist*. John Wiley & Sons, Ltd, 224(1), pp. 166–176. doi: 10.1111/NPH.15991.

Masutomi, Y. (2023) 'The appropriate analytical solution for coupled leaf photosynthesis and stomatal conductance models for C3 plants', *Ecological Modelling*. Elsevier B.V., 481(January), p. 110306. doi: 10.1016/j.ecolmodel.2023.110306.

Medlyn, B. E. *et al.* (2002) 'Temperature response of parameters of a biochemically based model of photosynthesis. II. A review of experimental data', *Plant, Cell and Environment*, 25(9), pp. 1167–1179. doi: 10.1046/j.1365-3040.2002.00891.x.

https://doi.org/10.5194/egusphere-2024-694
Preprint. Discussion started: 16 April 2024


Miller, J. D., Arteca, R. N. and Pell, E. J. (1999) 'Senescence-Associated Gene Expression during Ozone-Induced Leaf Senescence in Arabidopsis', *Plant Physiology*. Oxford University Press, 120(4), p. 1015. doi: 10.1104/PP.120.4.1015.

Muhie, S. H. (2022) 'Novel approaches and practices to sustainable agriculture', *Journal of Agriculture and Food Research*. Elsevier B.V., 10(August), p. 100446. doi: 10.1016/j.jafr.2022.100446.

Mulvaney, M. J. and Devkota, P. J. (2020) 'Adjusting Crop Yield to a Standard Moisture Content', *EDIS*. University of Florida George A Smathers Libraries, 2020(3). doi: 10.32473/EDIS-AG442-2020.

Nguyen, T. H. *et al.* (2024) 'Assessing the spatio-temporal tropospheric ozone and drought impacts on leaf growth and grain yield of wheat across Europe through crop modeling and remote sensing data', *European Journal of Agronomy*. Elsevier, 153, p. 127052. doi: 10.1016/J.EJA.2023.127052.

Van Oijen, M. and Ewert, F. (1999) 'The effects of climatic variation in Europe on the yield response of spring wheat cv. Minaret to elevated CO2 and O3: an analysis of open-top chamber experiments by means of two crop growth simulation models', *European Journal of Agronomy*. Elsevier, 10(3–4), pp. 249–264. doi: 10.1016/S1161-0301(99)00014-3.

Osborne, S. *et al.* (2019) 'New insights into leaf physiological responses to ozone for use in crop Modelling', *Plants*, 8(4). doi: 10.3390/plants8040084.

Osborne, T. *et al.* (2015) 'JULES-crop: A parametrisation of crops in the Joint UK Land Environment Simulator', *Geoscientific Model Development*, 8(4), pp. 1139–1155. doi: 10.5194/gmd-8-1139-2015.

Pleijel, H. *et al.* (2007) 'Ozone risk assessment for agricultural crops in Europe: Further development of stomatal flux and flux–response relationships for European wheat and potato', *Atmospheric Environment*. Pergamon, 41(14), pp. 3022–3040. doi: 10.1016/J.ATMOSENV.2006.12.002.

Pury, D. G. G. D. E. and Earquhar, G. D. (1997) 'Simple scaling of photosynthesis from leaves to canopies without the errors of big-leaf models', pp. 537–557.

Qin, X. *et al.* (2015) 'Wheat yield improvements in China: Past trends and future directions', *Field Crops Research*. Elsevier B.V., 177, pp. 117–124. doi: 10.1016/j.fcr.2015.03.013.

Schauberger, B. *et al.* (2019) 'Global historical soybean and wheat yield loss estimates from ozone pollution considering water and temperature as modifying effects', *Agricultural and Forest Meteorology*, 265(October 2018), pp. 1–15. doi: 10.1016/j.agrformet.2018.11.004.

Sharkey, T. D. *et al.* (2007) 'Fitting photosynthetic carbon dioxide response curves for C3 leaves', *Plant, Cell and Environment*, 30(9), pp. 1035–1040. doi: 10.1111/j.1365-3040.2007.01710.x.

Sillmann, J. *et al.* (2021) 'Combined impacts of climate and air pollution on human health and agricultural productivity', *Environmental Research Letters*, 16(9). doi: 10.1088/1748-9326/ac1df8.

Simpson, D. *et al.* (2012) 'The EMEP MSC-W chemical transport model – Technical description', *Atmospheric Chemistry and Physics*, 12(16), pp. 7825–7865. doi: 10.5194/acp-12-7825-2012.

Singh Yadav, D. *et al.* (2020) 'Responses of an old and a modern Indian wheat cultivar to future O 3 level: Physiological, yield and grain quality parameters *'. doi: 10.1016/j.envpol.2020.113939.

Sitch, S. *et al.* (2007) 'Indirect radiative forcing of climate change through ozone effects on the land-carbon sink', 448. doi: 10.1038/nature06059.

Tao, F. *et al.* (2017) 'Effects of climate change, CO2 and O3 on wheat productivity in Eastern China, singly and in combination', *Atmospheric Environment*. Elsevier Ltd, 153, pp. 182–193. doi: 10.1016/j.atmosenv.2017.01.032.

https://doi.org/10.5194/egusphere-2024-694
Preprint. Discussion started: 16 April 2024


Thomson, A. M. *et al.* (no date) 'RCP4.5: a pathway for stabilization of radiative forcing by 2100'. doi: 10.1007/s10584-011-0151-4.

Triboi, E. and Triboi-Blondel, A. M. (2002) 'Productivity and grain or seed composition: A new approach to an old problem - Invited paper', *European Journal of Agronomy*, 16(3), pp. 163–186. doi: 10.1016/S1161-0301(01)00146-0.

Wang, Q. J. (1997) 'Using genetic algorithms to optimise model parameters', *Environmental Modelling and Software*. Elsevier Ltd, 12(1), pp. 27–34. doi: 10.1016/S1364-8152(96)00030-8.

Yang, L. *et al.* (no date) 'Mathematical Programming for Piecewise Linear Regression Analysis'.

Zhang, X. *et al.* (2023) 'First long-term surface ozone variations at an agricultural site in the North China Plain: Evolution under changing meteorology and emissions', *Science of The Total Environment*. Elsevier, 860, p. 160520. doi: 10.1016/J.SCITOTENV.2022.160520.

Zheng, B. *et al.* (2015) 'The APSIM-Wheat Module (7.5 R3008)', p. 44. Available at: https://www.apsim.info/documentation/model-documentation/crop-module-documentation/wheat/.

Zhu, X. *et al.* (2011) 'Effects of elevated ozone concentration on yield of four Chinese cultivars of winter wheat under fully open-air field conditions', *Global Change Biology*. John Wiley & Sons, Ltd, 17(8), pp. 2697–2706. doi: 10.1111/J.1365-2486.2011.02400.X.

Amthor, J. S. *et al.* (2019) 'Engineering strategies to boost crop productivity by cutting respiratory carbon loss', *Plant Cell*, 31(2), pp. 297–314. doi: 10.1105/tpc.18.00743.

Betzelberger, A. M. *et al.* (2012) 'Ozone exposure response for U.S. soybean cultivars: Linear reductions in photosynthetic potential, biomass, and yield', *Plant Physiology*. American Society of Plant Biologists, 160(4), pp. 1827–1839. doi: 10.1104/pp.112.205591.

Biswas, D. K. *et al.* (2008) 'Assessing the genetic relatedness of higher ozone sensitivity of modern wheat to its wild and cultivated progenitors/relatives', *Journal of experimental botany*. J Exp Bot, 59(4), pp. 951–963. doi: 10.1093/JXB/ERN022.

Brewster, C., Fenner, N. and Hayes, F. (2024) 'Chronic ozone exposure affects nitrogen remobilization in wheat at key growth stages', *Science of The Total Environment*. Elsevier B.V., 908(August 2023), p. 168288. doi: 10.1016/j.scitotenv.2023.168288.

Brewster, C., Hayes, F. and Fenner, N. (2019) 'Ozone Tolerance Found in Aegilops tauschii and Primary Synthetic Hexaploid Wheat', *Plants 2019, Vol. 8, Page 195*. Multidisciplinary Digital Publishing Institute, 8(7), p. 195. doi: 10.3390/PLANTS8070195.

Campbell, G.S., Norman, J. M. (1998) *An introduction to Environmental Biophysics*. Second. Springer.

Challinor, A. J. *et al.* (2014) 'A meta-analysis of crop yield under climate change and adaptation', *Nature Climate Change*, 4(4), pp. 287–291. doi: 10.1038/nclimate2153.

Clark, D. B. *et al.* (2011) 'The Joint UK Land Environment Simulator (JULES), model description – Part 2: Carbon fluxes and vegetation dynamics', *Geoscientific Model Development*, 4(3), pp. 701–722. doi: 10.5194/gmd-4-701-2011.

Danielsson, H. *et al.* (2003) 'Ozone uptake modelling and flux-response relationships - An assessment of ozone-induced yield loss in spring wheat', *Atmospheric Environment*. Pergamon, 37(4), pp. 475–485. doi: 10.1016/S1352-2310(02)00924-X.

https://doi.org/10.5194/egusphere-2024-694
Preprint. Discussion started: 16 April 2024


Emberson, L.D., Ashmore, M.R., Simpson, D., Tuovinen, J.-P. and Cambridge, H. M. (2001) 'Modelling and mapping ozone deposition in Europe', *Water, Air and Soil Pollution*, pp. 577–582.

Emberson, L. D. *et al.* (2000) 'Modelling stomatal ozone flux across Europe', *Environmental Pollution*, 109(3), pp. 403–413. doi: 10.1016/S0269-7491(00)00043-9.

Emberson, L. D. *et al.* (2018) 'Ozone effects on crops and consideration in crop models', *European Journal of Agronomy*. Elsevier, 100(May), pp. 19–34. doi: 10.1016/j.eja.2018.06.002.

Ewert, F. and Porter, J. R. (2000) 'Ozone effects on wheat in relation to CO2: Modelling short-term and long-term responses of leaf photosynthesis and leaf duration', *Global Change Biology*, 6(7), pp. 735–750. doi: 10.1046/j.1365-2486.2000.00351.x.

Farage, P. K. *et al.* (1991) 'The sequence of change within the photosynthetic apparatus of wheat following short-term exposure to ozone', *Plant Physiology*, 95(2), pp. 529–535. doi: 10.1104/pp.95.2.529.

Farquhar, G.D., von Caemmerer, S., Berry, J. A. (1980) 'A biochemical model of photosynthetic CO2 assimilation in leaves of C3 species', *Planta*, 149, pp. 78–90.

Farquhar, G. D., Caemmerer, S. and Berry, J. A. (1980) 'A biochemical model of photosynthetic $CO_2$ assimilation in leaves of $C_3$ species', *Planta*, 149(1), pp. 78-90–90. Available at: http://dx.doi.org/10.1007/BF00386231.

Feng, Y. *et al.* (2022) 'Identifying and modelling key physiological traits that confer tolerance or sensitivity to ozone in winter wheat', *Environmental Pollution*. Elsevier Ltd, 304(April), p. 119251. doi: 10.1016/j.envpol.2022.119251.

Feng, Y. *et al.* (2024) 'Alteration of carbon and nitrogen allocation in winter wheat under elevated ozone', *Plant Science*. Elsevier, 338, p. 111924. doi: 10.1016/J.PLANTSCI.2023.111924.

Feng, Z. *et al.* (2011) 'Differential responses in two varieties of winter wheat to elevated ozone concentration under fully open-air field conditions', *Global Change Biology*, 17(1), pp. 580–591. doi: 10.1111/J.1365-2486.2010.02184.X.

Feng, Z. *et al.* (2012) 'A stomatal ozone flux-response relationship to assess ozone-induced yield loss of winter wheat in subtropical China', *Environmental Pollution*. Elsevier Ltd, 164, pp. 16–23. doi: 10.1016/j.envpol.2012.01.014.

Feng, Z. *et al.* (2016) 'Differential effects of ozone on photosynthesis of winter wheat among cultivars depend on antioxidative enzymes rather than stomatal conductance', *The Science of the total environment*. Sci Total Environ, 572, pp. 404–411. doi: 10.1016/J.SCITOTENV.2016.08.083.

Feng, Z. *et al.* (2018) 'Comparison of crop yield sensitivity to ozone between open-top chamber and free-air experiments', *Global Change Biology*. Blackwell Publishing Ltd, 24(6), pp. 2231–2238. doi: 10.1111/gcb.14077.

Feng, Z. *et al.* (2021) 'Emerging challenges of ozone impacts on asian plants: actions are needed to protect ecosystem health'. doi: 10.1080/20964129.2021.1911602.

Feng, Z., Kobayashi, K. and Ainsworth, E. A. (2008) 'Impact of elevated ozone concentration on growth, physiology, and yield of wheat (Triticum aestivum L.): A meta-analysis', *Global Change Biology*, 14(11), pp. 2696–2708. doi: 10.1111/j.1365-2486.2008.01673.x.

Gelang, J. *et al.* (2000) 'Rate and duration of grain filling in relation to flag leaf senescence and grain yield in spring wheat (Triticum aestivum) exposed to different concentrations of ozone', *Physiologia Plantarum*, 110(3), pp. 366–375. doi: 10.1111/J.1399-3054.2000.1100311.X.

https://doi.org/10.5194/egusphere-2024-694
Preprint. Discussion started: 16 April 2024


Graham, A. M. *et al.* (2020) 'Impact on air quality and health due to the Saddleworth Moor fire in northern England', *Environmental Research Letters*, 15(7). doi: 10.1088/1748-9326/ab8496.

Graham, A. M. *et al.* (2021) 'Impact of the 2019/2020 Australian Megafires on Air Quality and Health', *GeoHealth*, 5(10), pp. 1–17. doi: 10.1029/2021GH000454.

Grandjean, A. and Fuhrer Grandjean, J. (1989) *Growth and leaf senescence in spring wheat (Triticum aestivum) grown at different ozone concentrations in open-top field chambers*.

Guan, X. K. *et al.* (2015) 'Effect of Drought on the Gas Exchange, Chlorophyll Fluorescence and Yield of Six Different-Era Spring Wheat Cultivars', *Journal of Agronomy and Crop Science*, 201(4), pp. 253–266. doi: 10.1111/jac.12103.

Huang, H. *et al.* (2022) 'A dataset of winter wheat aboveground biomass in China during 2007–2015 based on data assimilation', *Scientific Data*. Springer US, 9(1), pp. 1–11. doi: 10.1038/s41597-022-01305-6.

Jaggi, M. *et al.* (2006) 'Environmental control of profiles of ozone concentration in a grassland canopy', *Atmospheric Environment*, 40(28), pp. 5496–5507. doi: 10.1016/j.atmosenv.2006.01.025.

Jones, H. G. (1992) *Plants and microclimate: A quamntitative approach to environmental plant physiology*. Cambridge University Press.

Kohut, R. J., Amundson, R. G. and Laurence, J. A. (1987) 'Effects of ozone and sulfur dioxide on yield of winter wheat', *Phytopathology*, 77(1), pp. 71–74. doi: 10.1094/Phyto-77-71.

Konduri, V. S. *et al.* (2020) 'Data Science for Weather Impacts on Crop Yield', *Frontiers in Sustainable Food Systems*, 4(May). doi: 10.3389/fsufs.2020.00052.

Lee, J. D. *et al.* (2020) 'UK surface NO2 levels dropped by 42 % during the COVID-19 lockdown: Impact on surface O3', *Atmospheric Chemistry and Physics*, 20(24), pp. 15743–15759. doi: 10.5194/acp-20-15743-2020.

Leung, F. *et al.* (2020) 'Calibrating soybean parameters in JULES 5.0 from the US-Ne2/3 FLUXNET sites and the SoyFACE-O3 experiment', *Geoscientific Model Development*. Copernicus GmbH, 13(12), pp. 6201–6213. doi: 10.5194/GMD-13-6201-2020.

Leuning, R. (1990) 'MODELING STOMATAL BEHAVIOR AND PHOTOSYNTHESIS OF EUCALYPTUS-GRANDIS', *AUSTRALIAN JOURNAL OF PLANT PHYSIOLOGY*, 17(2), pp. 159–175.

Leuning, R. (1995) 'A critical appraisal of combine stomatal model C3 plants', *Plant, Cell & Environment*, 18, pp. 339–355. Available at: http://www.unc.edu/courses/2010spring/geog/595/001/www/Leuning95b-PCE.pdf%0Apapers2://publication/uuid/B8B998AB-EB42-4E09-A609-B192084D13EE.

Li, A., Zhou, Q. and Xu, Q. (2021) 'Prospects for ozone pollution control in China: An epidemiological perspective', *Environmental Pollution*. Elsevier Ltd, 285. doi: 10.1016/J.ENVPOL.2021.117670.

Li, D. *et al.* (2022) 'Surface ozone impacts on major crop production in China from 2010 to 2017', *Atmospheric Chemistry and Physics*, 22(4), pp. 2625–2638. doi: 10.5194/acp-22-2625-2022.

Li, K. *et al.* (2020) 'anthropogenic and meteorological influences', *Atmos. Chem. Phys*, 20, pp. 11423–11433. doi: 10.5194/acp-20-11423-2020.

Lin, M. *et al.* (2017) 'US surface ozone trends and extremes from 1980 to 2014: Quantifying the roles of rising Asian emissions, domestic controls, wildfires, and climate', *Atmospheric Chemistry and Physics*, 17(4), pp. 2943–2970. doi: 10.5194/acp-17-2943-2017.

https://doi.org/10.5194/egusphere-2024-694
Preprint. Discussion started: 16 April 2024


Liu, S. *et al.* (2010) 'Crop yield responses to climate change in the Huang-Huai-Hai Plain of China', *Agricultural Water Management*. Elsevier, 97(8), pp. 1195–1209. doi: 10.1016/J.AGWAT.2010.03.001.

Liu, Z. *et al.* (2022) 'Tropospheric ozone changes and ozone sensitivity from the present day to the future under shared socio-economic pathways', *Atmospheric Chemistry and Physics*. Copernicus GmbH, 22(2), pp. 1209–1227. doi: 10.5194/ACP-22-1209-2022.

Malhi, G. S., Kaur, M. and Kaushik, P. (2021) 'Impact of Climate Change on Agriculture and Its Mitigation Strategies: A Review', *Sustainability 2021, Vol. 13, Page 1318*. Multidisciplinary Digital Publishing Institute, 13(3), p. 1318. doi: 10.3390/SU13031318.

Mariën, B. *et al.* (2019) 'Detecting the onset of autumn leaf senescence in deciduous forest trees of the temperate zone', *New Phytologist*. John Wiley & Sons, Ltd, 224(1), pp. 166–176. doi: 10.1111/NPH.15991.

Masutomi, Y. (2023) 'The appropriate analytical solution for coupled leaf photosynthesis and stomatal conductance models for C3 plants', *Ecological Modelling*. Elsevier B.V., 481(January), p. 110306. doi: 10.1016/j.ecolmodel.2023.110306.

Medlyn, B. E. *et al.* (2002) 'Temperature response of parameters of a biochemically based model of photosynthesis. II. A review of experimental data', *Plant, Cell and Environment*, 25(9), pp. 1167–1179. doi: 10.1046/j.1365-3040.2002.00891.x.

Miller, J. D., Arteca, R. N. and Pell, E. J. (1999) 'Senescence-Associated Gene Expression during Ozone-Induced Leaf Senescence in Arabidopsis', *Plant Physiology*. Oxford University Press, 120(4), p. 1015. doi: 10.1104/PP.120.4.1015.

Muhie, S. H. (2022) 'Novel approaches and practices to sustainable agriculture', *Journal of Agriculture and Food Research*. Elsevier B.V., 10(August), p. 100446. doi: 10.1016/j.jafr.2022.100446.

Mulvaney, M. J. and Devkota, P. J. (2020) 'Adjusting Crop Yield to a Standard Moisture Content', *EDIS*. University of Florida George A Smathers Libraries, 2020(3). doi: 10.32473/EDIS-AG442-2020.

Nguyen, T. H. *et al.* (2024) 'Assessing the spatio-temporal tropospheric ozone and drought impacts on leaf growth and grain yield of wheat across Europe through crop modeling and remote sensing data', *European Journal of Agronomy*. Elsevier, 153, p. 127052. doi: 10.1016/J.EJA.2023.127052.

Van Oijen, M. and Ewert, F. (1999) 'The effects of climatic variation in Europe on the yield response of spring wheat cv. Minaret to elevated CO2 and O3: an analysis of open-top chamber experiments by means of two crop growth simulation models', *European Journal of Agronomy*. Elsevier, 10(3–4), pp. 249–264. doi: 10.1016/S1161-0301(99)00014-3.

Osborne, S. *et al.* (2019) 'New insights into leaf physiological responses to ozone for use in crop Modelling', *Plants*, 8(4). doi: 10.3390/plants8040084.

Osborne, T. *et al.* (2015) 'JULES-crop: A parametrisation of crops in the Joint UK Land Environment Simulator', *Geoscientific Model Development*, 8(4), pp. 1139–1155. doi: 10.5194/gmd-8-1139-2015.

Pleijel, H. *et al.* (2007) 'Ozone risk assessment for agricultural crops in Europe: Further development of stomatal flux and flux–response relationships for European wheat and potato', *Atmospheric Environment*. Pergamon, 41(14), pp. 3022–3040. doi: 10.1016/J.ATMOSENV.2006.12.002.

Pury, D. G. G. D. E. and Earquhar, G. D. (1997) 'Simple scaling of photosynthesis from leaves to canopies without the errors of big-leaf models', pp. 537–557.

Qin, X. *et al.* (2015) 'Wheat yield improvements in China: Past trends and future directions', *Field Crops Research*. Elsevier B.V., 177, pp. 117–124. doi: 10.1016/j.fcr.2015.03.013.

https://doi.org/10.5194/egusphere-2024-694
Preprint. Discussion started: 16 April 2024


Schauberger, B. *et al.* (2019) 'Global historical soybean and wheat yield loss estimates from ozone pollution considering water and temperature as modifying effects', *Agricultural and Forest Meteorology*, 265(October 2018), pp. 1–15. doi: 10.1016/j.agrformet.2018.11.004.

Sharkey, T. D. *et al.* (2007) 'Fitting photosynthetic carbon dioxide response curves for C3 leaves', *Plant, Cell and Environment*, 30(9), pp. 1035–1040. doi: 10.1111/j.1365-3040.2007.01710.x.

Sillmann, J. *et al.* (2021) 'Combined impacts of climate and air pollution on human health and agricultural productivity', *Environmental Research Letters*, 16(9). doi: 10.1088/1748-9326/ac1df8.

Simpson, D. *et al.* (2012) 'The EMEP MSC-W chemical transport model – Technical description', *Atmospheric Chemistry and Physics*, 12(16), pp. 7825–7865. doi: 10.5194/acp-12-7825-2012.

Singh Yadav, D. *et al.* (2020) 'Responses of an old and a modern Indian wheat cultivar to future O 3 level: Physiological, yield and grain quality parameters *'. doi: 10.1016/j.envpol.2020.113939.

Sitch, S. *et al.* (2007) 'Indirect radiative forcing of climate change through ozone effects on the land-carbon sink', 448. doi: 10.1038/nature06059.

Tao, F. *et al.* (2017) 'Effects of climate change, CO2 and O3 on wheat productivity in Eastern China, singly and in combination', *Atmospheric Environment*. Elsevier Ltd, 153, pp. 182–193. doi: 10.1016/j.atmosenv.2017.01.032.

Thomson, A. M. *et al.* (no date) 'RCP4.5: a pathway for stabilization of radiative forcing by 2100'. doi: 10.1007/s10584-011-0151-4.

Triboi, E. and Triboi-Blondel, A. M. (2002) 'Productivity and grain or seed composition: A new approach to an old problem - Invited paper', *European Journal of Agronomy*, 16(3), pp. 163–186. doi: 10.1016/S1161-0301(01)00146-0.

Wang, Q. J. (1997) 'Using genetic algorithms to optimise model parameters', *Environmental Modelling and Software*. Elsevier Ltd, 12(1), pp. 27–34. doi: 10.1016/S1364-8152(96)00030-8.

Yang, L. *et al.* (no date) 'Mathematical Programming for Piecewise Linear Regression Analysis'.

Zhang, X. *et al.* (2023) 'First long-term surface ozone variations at an agricultural site in the North China Plain: Evolution under changing meteorology and emissions', *Science of The Total Environment*. Elsevier, 860, p. 160520. doi: 10.1016/J.SCITOTENV.2022.160520.

Zheng, B. *et al.* (2015) 'The APSIM-Wheat Module (7.5 R3008)', p. 44. Available at: https://www.apsim.info/documentation/model-documentation/crop-module-documentation/wheat/.

Zhu, X. *et al.* (2011) 'Effects of elevated ozone concentration on yield of four Chinese cultivars of winter wheat under fully open-air field conditions', *Global Change Biology*. John Wiley & Sons, Ltd, 17(8), pp. 2697–2706. doi: 10.1111/J.1365-2486.2011.02400.X.